Economic Analysis for In-Situ Resource Utilization on Mars in Support of the Generation of Rocket Fuel and Potable Water

A Technical Report submitted to the Department of Chemical Engineering

Presented to the Faculty of the School of Engineering and Applied Science
University of Virginia • Charlottesville, Virginia

In Partial Fulfillment of the Requirements for the Degree
Bachelor of Science, School of Engineering

Spring 2022

Technical Project Team Members:

Hannah Alexander

Donovan Hensley

Lessanu Mequanint

Cameron Tanaka

On my honor as a University Student, I have neither given nor received unauthorized aid on this assignment as defined by the Honor Guidelines for Thesis-Related Assignments

Eric Anderson, Department of Chemical Engineering

TABLE OF CONTENTS

1. Executive Summary

In-situ resource utilization (ISRU) can help to reduce the costs associated with interplanetary manned missions. This is possible because the highest costs for space missions are the liftoff costs, amounting to roughly $10,000 per pound sent into space (Boen, 2008). To combat the high price associated with manned Mars missions, generating rocket fuel on Mars for a return trip was researched. Our process uses ice on Mars to generate hydrogen through electrolysis and subsequently takes carbon dioxide from the atmosphere to produce methane and potable water through a Sabatier reaction. Oxygen is also produced from electrolysis, ultimately acting as an oxidizer for the methane being used as rocket fuel. 7.2 tons of methane and 28.8 tons of oxygen are produced in an 8-month window to support a low energy return trip for the astronauts. Our system was modeled using Aspen simulations, combined with detailed equipment designs for such units as the Sabatier reactor and the heat exchangers. This system is powered by Kilopower generators, which utilize nuclear fission to generate electricity. The longevity of our plant was not fully researched but it is known to be able to endure three cycles with minimal replacement of parts for cheap consumables like catalysts. Shipping rocket fuel from Earth would cost about $720 million. Overall, our process is estimated to cost $805 million for one round trip if the potable water produced is not considered at all. If it is considered in terms of its liftoff cost being conserved, the mission would save $238 million. If two cycles used the system without water, the savings would be $564 million. If water was considered as well, the savings would be $1.2 billion. Thus, if more than one mission for Mars is planned, or water plays a large role in any other Martian system, ISRU should be utilized in this manner. Some areas for improvement include reducing energy consumption as the Kilopower units are responsible for some of the greatest costs for the system. Overall, our proposed process intends

to contribute to research related to ISRU as well as interplanetary pursuits through manned missions on the whole.

2. Background and Motivation

2.1 Background

The inspiration for our project stems from proposals of extraterrestrial exploration dating back to the mid-20th century. For example, in-situ propellant production on Mars was first conceptualized in the early 1960s (Portree, 2013). However, it was not until President George H. W. Bush's introduction of the Space Exploration Initiative (SEI) in July 1989 and the associated establishment of NASA's Outreach Program that an abundance of Mars mission plans were developed (Portree, 2013). In particular, the Outreach Program compiled over 2,000 ideas for executing such goals of the SEI as surveying Mars, the most notable of which is Mars Direct (Portree, 2013).

Robert Zubrin and David Baker, the engineers responsible for Mars Direct, presented their plan to NASA in April 1990 and to the public during the subsequent month (Portree, 2013). While NASA was intrigued by Mars Direct, it noted critical complications within the proposal, including the insufficient size of the Earth Return Vehicle (ERV) cabin for a crew of four astronauts and the potential for rover occupants to become stranded while exploring (Portree, 2013). In 1994, NASA also estimated that the actualization of Mars Direct would require $50 billion (Zubrin, 2000). In spite of these factors, Robert Zubrin has expanded upon the initial version of Mars Direct and continued to passionately advocate for the plan in the years since.

An iteration of Mars Direct that was published in 2000 delineates the necessities of traveling light and living off the land (Zubrin, 2000). Specifically, the plan would include a booster rocket whose upper stage detaches for the purpose of heaving a 45-metric-ton unmanned payload, referred to as the ERV, on a trajectory to Mars such that preparations could be made in advance of the arrival of astronauts two years later (Zubrin, 2000). The ERV would transport

liquid-hydrogen cargo, compressors, a chemical-processing unit, small rovers, and a 100-kilowatt nuclear reactor attached to a large rover fueled by a mixture of methane and oxygen (Zubrin, 2000). The chemical-processing unit would generate the products of methane and water via the reduction of carbon dioxide from the Martian atmosphere by hydrogen brought from Earth (Zubrin, 2000). The water would be electrolyzed such that hydrogen and oxygen result, with the former fed into the chemical-processing unit and the latter saved for later use (Zubrin, 2000). A total of 108 tons of methane-oxygen propellant would be produced over the course of eight months, which equates to 18 times the quantity of original feedstock (Zubrin, 2000). Our project draws from Mars Direct in a number of ways, especially through reliance on methanation and electrolysis, as will be made apparent in the process discussion to follow.

Since Mars Direct was originally proposed, plans for Mars missions have evolved in response to discoveries made through research efforts on the planet. Of particular significance, NASA's Phoenix Mars lander detected solid water on Mars in June 2008 (*NASA Phoenix*, 2008). As such, the capabilities of in-situ resource utilization (ISRU) on the planet have expanded to include ice. This progression has also been reflected in capstone projects completed by former chemical engineering majors at the University of Virginia, some of the most recent of which have informed our project. One such work that was published in May 2020 has primarily guided our project as it was developed using contemporary knowledge of the conditions on Mars. However, our project involves methane generated via the Sabatier reaction for fuel, whereas this function is supported by hydrogen generated via the water-gas shift reaction in the referenced literature (Mace et al., 2020).

2.2 Motivation

While extraterrestrial exploration has been discussed for decades, the announcement of SpaceX's Mars mission has increased interest lately. Recent discoveries via NASA's Mars Exploration Program have also seemingly boosted the likelihood of colonizing the planet. Specifically, in September 2021 NASA's Perseverance rover discovered basaltic rocks on Mars that indicate lengthy eras marked by volcanic activity and groundwater on a planet previously believed to be barren of essential resources (*NASA's Perseverance*, 2021). Space exploration is compelling overall because the settlement of other planets would advance humanity's understanding of the entire universe.

Modern economic incentives for industrialization of a colony on Mars have also motivated the investigation of this project. A 2013 NASA report states that the space agency enhanced the competitiveness of, spurred innovation and growth in, and created employment opportunities in the technology and manufacturing fields (Dallas et al., 2020). Advancements in communication, internet, weather prediction, and GPS are reliant on the development of space technologies, benefiting the economy through the resultant job creation. In 2019 alone, NASA supported more than 312,000 jobs, generated $7 billion in taxes, and created $64.3 billion in total economic output (Inclán et al., 2020). Innovations driven by the heightened competition surrounding Mars exploration will likely increase these numbers.

2.3 Products

The goal of our project is to determine if it is more economically viable to create rocket fuel and store it in-situ on Mars than to ship it from Earth. Generating potable water serves as a secondary objective as water is a byproduct of rocket fuel creation. Our team considered the following two fuel options: hydrogen produced from the water-gas shift reaction and methane produced from the Sabatier reaction. Ultimately, methane was selected as the fuel source for our project due to the fact that meaningful volumes of the material can be stored by liquefying the compound at -238 ^{o}F at 14.7 psia, while hydrogen liquefies at the much lower value of -423 ^{o}F at 14.7 psia (National Center for Biotechnical Information, 2021). Given the temperatures typical of Mars' atmosphere, this property of methane makes it easier to manage than hydrogen as a rocket fuel.

Due to the use of methane of 99.5% purity in an investigation simulating the conditions found in rocket nozzle cooling channels, we chose to produce methane of the same quality for our project (Heldens et al., 2021). Furthermore, as water is to be consumed by the astronauts, the water generated is of nearly 100% purity to ensure potability. In the Sabatier reaction that follows, the reactants of carbon dioxide and hydrogen are denoted by CO_2 and H_2, respectively, while the products of methane and water are denoted by CH_4 and H_2O, respectively (Blauth et al., 2021):

$$CO_2 + 4H_2 \rightleftharpoons CH_4 + 2H_2O$$

It is customary for liquid oxygen to be used in rocket engines, therefore oxygen principally serves as an oxidizer for methane in our project (*Propellants*, n.d.). This role typically involves liquid oxygen of 99.5% purity (Wade, n.d.). Oxygen, denoted by O_2, is produced

through electrolysis via the following reaction, where hydrogen is an additional product and water is the sole reactant (*Hydrogen Production*, n.d.):

$$2H_2O \rightarrow 2H_2 + O_2$$

2.4 Starting Materials

To make the desired products, the necessary materials for the feed streams are readily available on Mars. On the other hand, the materials required for the reactors need to be transported from Earth. The atmosphere of Mars is mostly carbon dioxide. According to NASA's Sample Analysis at Mars, the atmosphere is composed of about 95% carbon dioxide, 2.6% nitrogen gas, 1.9% argon, 0.16% oxygen gas, and 0.06% carbon monoxide (Shekhtman, 2019). The prevalence of carbon dioxide in the air ensures that there is enough of this material readily available for our process. Feeding Martian air into a separator can isolate carbon dioxide from the other materials present in the atmosphere.

The water required for this process is slightly more difficult to collect and purify than the carbon dioxide, yet it is still readily available below the surface of Mars in the solid form. Ice can be found in the regolith of Mars, which is a layer of porous soil (Niels Bohr Institute, n.d.). Using an ice drilling machine is the most practical and cost-effective method for extracting the necessary materials as this approach avoids the requirement for human labor, which is scarce and expensive on Mars. In order to use the resources on Mars most effectively, NASA plans to send many autonomous devices to mine the planet's surface and has already been researching and conducting competitions to explore this technology (Xsens, n.d.). For our process, we have decided to use Honeybee's AutoGopher II ice drilling machine to extract ice from the regolith. This is because it is highly efficient, the technology is mature, and the materials are relatively light. This machine requires less than 500 W to run and it weighs 143.3 lb. The design of this machine will be outsourced to mechanical engineers and is out of the scope of this process. Nuclear generators can be used to power this robot because they are flight-proven to be safe and reliable for power generation in space (Dudzinski, n.d.). The ice taken from the soil needs to be

melted with a heat exchanger. The water collected from the soil is not pure, and salts like perchlorate, sulfate, sodium, potassium, and calcium ions are removed during the process with a desalination unit. According to a past capstone project, the assumed composition of this water mixture on Mars after liquefaction is displayed in Table 2.4.1 (Mace et al., 2020, p. 18).

Table 2.4.1. Assumed Composition of Liquefied Martian Water Mixture

Component	Weight Percent
H_2O	82.50
$MgSO_4$	5.75
Na_2SO_4	5.75
$MgCO_3$	2.50
$CaCO_3$	2.50
NaCl	1.00

Using a Sabatier reactor is appealing for long-term space exploration applications. The apparatus has been proven to effectively recover water on the International Space Station and a prototype was able to produce methane in a simulated Martian environment (Vogt et al., 2019). Currently, NASA is investigating catalysts that are compatible with the materials found in Mars' atmosphere (Vogt et al., 2019). Nickel aluminum oxide catalysts have been demonstrated for applications on Earth due to their strong ability for methanation and cost-effectiveness (Junaedi et al., 2011; Vogt et al., 2019). However, at temperatures of less than 572 ^{o}F, nickel is more likely to be deactivated by oxidation and form $Ni(CO)_4$, which is highly toxic (Vogt et al., 2019). On the other hand, ruthenium catalysts are more durable than nickel materials so they are usually chosen for Sabatier reactors in space, despite being about two to three times more expensive than nickel catalysts (Moioli & Züttel, 2020). One study compared the performance of a nickel-based

catalyst (SNG 8000) and different ruthenium catalysts (0.5% Ru and 2.0% Ru), using aluminum oxide as the inner packing material and Acros glass wool as the outer packing material (Franco et al., 2019). They contrasted baseline reactors and test cases that examined the effects of vibration, liquid water exposure, and particle and chemical contamination (Franco et al., 2019). This comparison aimed to simulate the conditions on Mars and the vibrations caused by launching these materials into space, ultimately finding that all of the catalysts performed well and did not deviate significantly in terms of methane production (Franco et al., 2019). Based on the aforementioned reasons, our process uses a ruthenium catalyst. To save on ruthenium costs, we employ a 0.5% Ru catalyst, as it showed similar results to the 2.0% Ru catalyst.

2.5 Process Overview

The production of methane, water, and oxygen requires a system of unit operations to convert initial starting materials and separate final products. Martian ice and atmospheric gases are fed through a series of operations such as an atmosphere separator, a desalination unit, and an electrolyzer before the desired components are fed into secondary units like the Sabatier reactor, dehumidifier, and a cryogenic distillation column, as illustrated in Figure 2.5.1. This process requires several storage tanks, which are designed according to their contents, holding time, and volumetric flow rate. However, product storage tanks were excluded from our analysis as shipping rocket fuel from Earth would require the same elements. Additionally, the orbits of Earth and Mars dictate the available time frame for producing enough rocket fuel for the return trip (Williams, 2015). One launch window cycle lasts approximately 26 months with each leg of the journey requiring 9 months of travel; this amounts to 8 months on Mars, which is a feasible period for generating rocket fuel and potable water (Redd, 2017).

The desired mass of the methane and liquid oxygen mixture to be generated for this process is 36 tons. Multiple sources indicate that 4 times as much oxygen by mass, or a 2 to 1 molar ratio of fuel to oxidizer, would be needed for the return trip (Kruyer et al., 2021; *SpaceX Raptor*, n.d.). Producing excess oxygen in this process mitigates losses due to evaporation (Mace et al., 2020). We also include a safety factor of 1.2 to further account for the potential for these materials to evaporate. Therefore, 7.2 tons of methane and 28.8 tons of oxygen are produced by this process, which was found by multiplying the total requirements by 1.2.

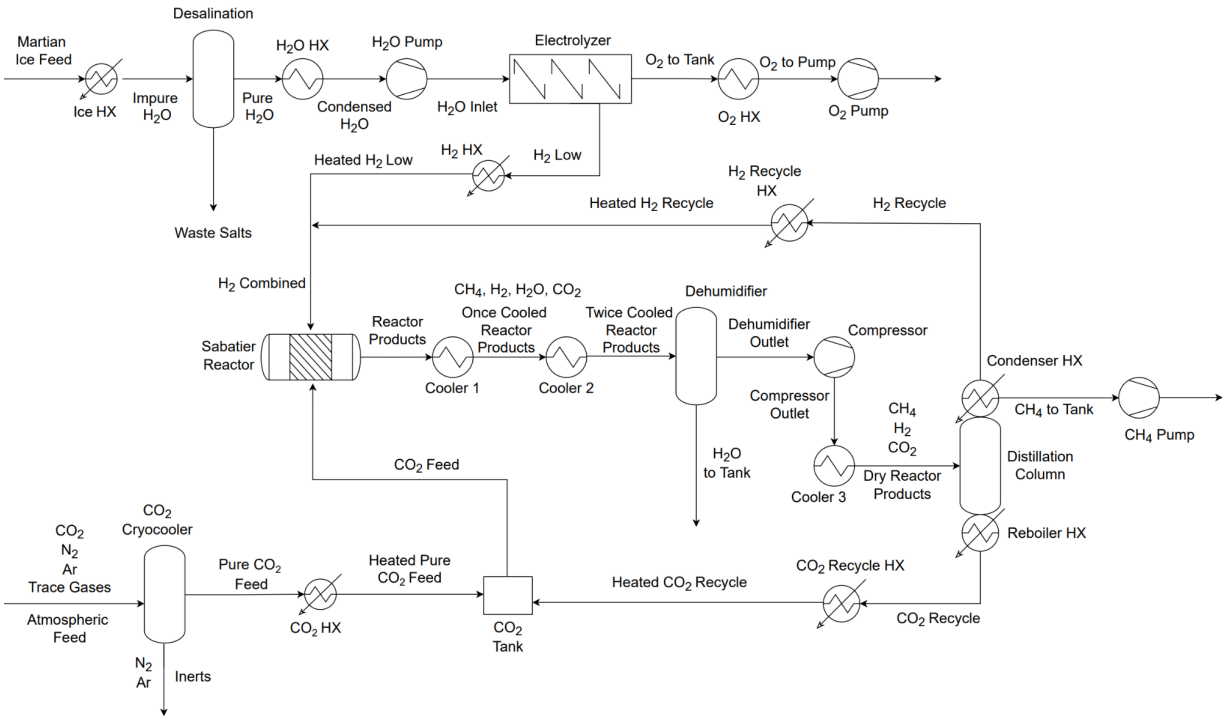

Figure 2.5.1. Full Process Flow Diagram with Stream Names for Mars ISRU Process

3. Process Design Discussion

For many of the pieces of equipment to be discussed, process design specifications are characterized by custom fabrication rather than sizes commonly found in industry. While this is generally an expensive practice up front, such a reliance on custom fabrication is justified by the significance of mass in our project. For example, savings on liftoff costs, which directly correlate to mass, are likely greater than those afforded by sizing up to the next schedule of piping.

3.1 Atmosphere Separation

Our feed separation unit freezes carbon dioxide in order to separate it from other gases found in the atmosphere to be fed into our process at roughly 100% purity. The estimated atmospheric composition of Mars is displayed in Table 3.1.1 (Meier et al., 2018).

Table 3.1.1. Approximate Atmospheric Composition of Mars on a Volume Basis

Component	**Percent of Martian atmosphere (volume basis)**
CO_2	95.33
N_2	2.70
Ar	1.60
Trace gases (O_2 & CO)	0.37

Estimating an average temperature and pressure on Mars, the atmospheric composition on a mass basis was calculated with Aspen, and is shown in Table 3.1.2.

Table 3.1.2. Approximate Atmospheric Composition of Mars on a Mass Basis

Component	**Percent of Martian atmosphere (mass basis)**
CO_2	96.78
N_2	1.74
Ar	1.47
Trace gases (O_2 & CO)	0.01

We initially planned to use a pressure-swing adsorber with Lithium X zeolites to remove nitrogen and argon from the atmospheric feed, which would use two columns with changing

pressures to create a continuous separating system (*Molecular Sieves*, n.d.; Pan et al., 2017). However, based on existing literature comparing many forms of technology that could serve this purpose (i.e., freezing, membrane separation, ionic liquids, acid-base chemistry, molecular sieves, and other types of preparative chromatography), we decided that freezing would be the most promising approach due to its relative simplicity and the fact that it is well understood, as well as its ability to produce high purity carbon dioxide at high pressures (Devor et al., 2014). We based our design off a full-scale cryogenic carbon dioxide freezer design that can produce 2.14 lb/hr of pure carbon dioxide (Meier et al., 2018). Carbon monoxide and oxygen were not considered for this process as even if they were to freeze with the carbon dioxide, they would not affect our process as carbon monoxide is an intermediate in our methanation reaction and oxygen would produce water in that reactor, which is separated from the other materials in the desalination unit. The unit is 3.13 ft in length, 1.50 ft in width, 2.08 ft in height, and it weighs 340 lb (Meier et al., 2018). The input and output flow rates are displayed in Table 3.1.3 below, assuming the lower end for efficiency for freezing carbon dioxide, that being 71%, from the design of Meier et al.

Table 3.1.3. Atmospheric Separator Unit Inlet and Outlet Flow Rates

Streams	**Atmospheric Feed**	**Inerts**	**Pure CO_2 Feed**
CO_2 (lb/hr)	11.18	3.24	7.94
N_2 (lb/hr)	0.127	0.127	0.000
Ar (lb/hr)	0.154	0.154	0.000

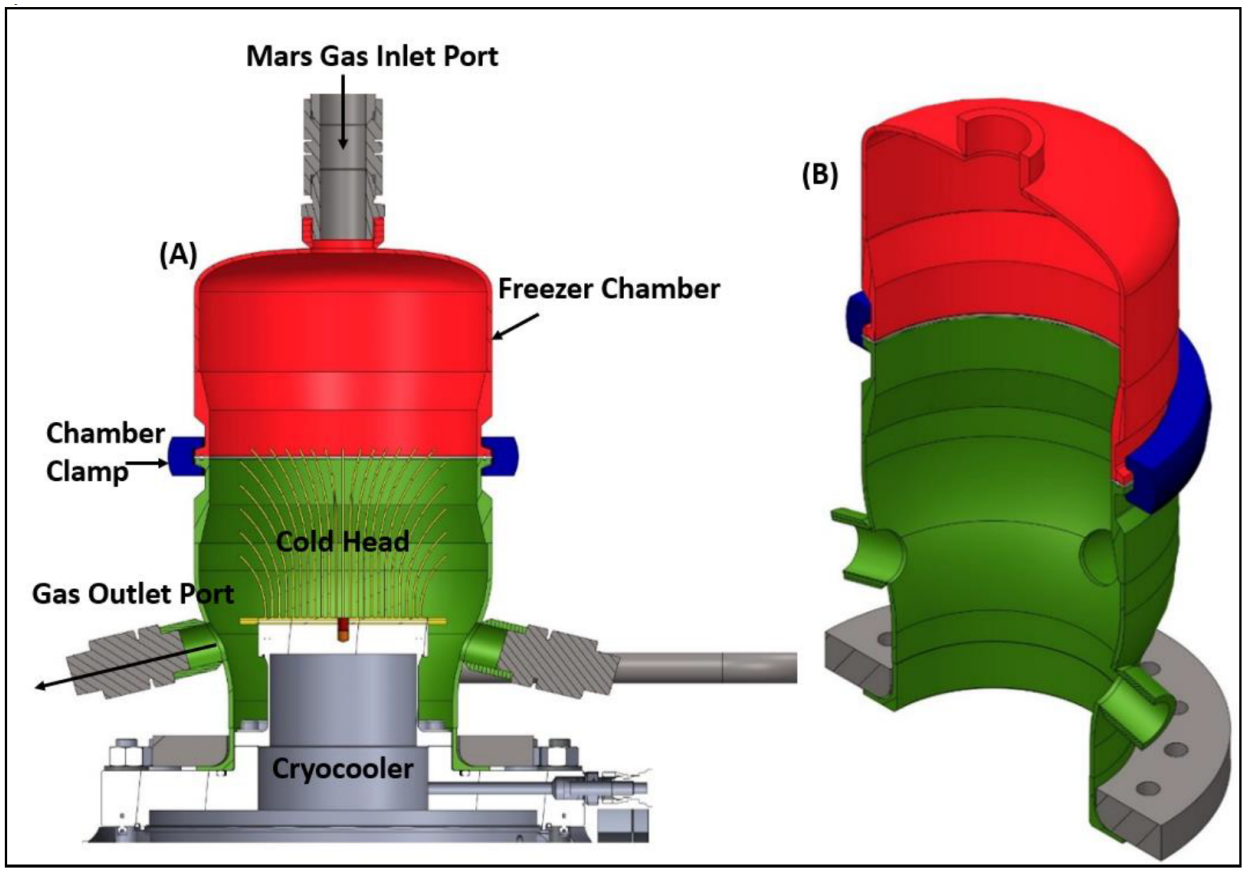

Figure 3.1.1. Carbon Dioxide Freezer Unit Design (Meier et al., 2018)

To meet our design requirement of 7.94 lb/hr, we would need 4 of their units, one of which is displayed in Figure 3.1.1. Also, the team designing these units considered components that would allow for a minimum operating time of about 14 months without maintenance, which is considerably longer than the 8 months we are targeting for the operation of our unit (Meier et al., 2018). Their design sends air from Mars at its atmospheric pressure and temperature, which was estimated to be 0.116 psi and -63.67 ℉, into a carbon dioxide freezer chamber using a fan (Meier et al., 2018). Their design is made to accommodate various operating pressures and temperatures, so we chose our conditions based on the approximate center of their operating envelope (Meier et al., 2018). An AFCryo STC90 cryocooler then removes heat from the freezer

chamber using thermal contact with a Stirling cold head. The design of this system is shown in Figure 3.1.2 (Meier et al., 2018).

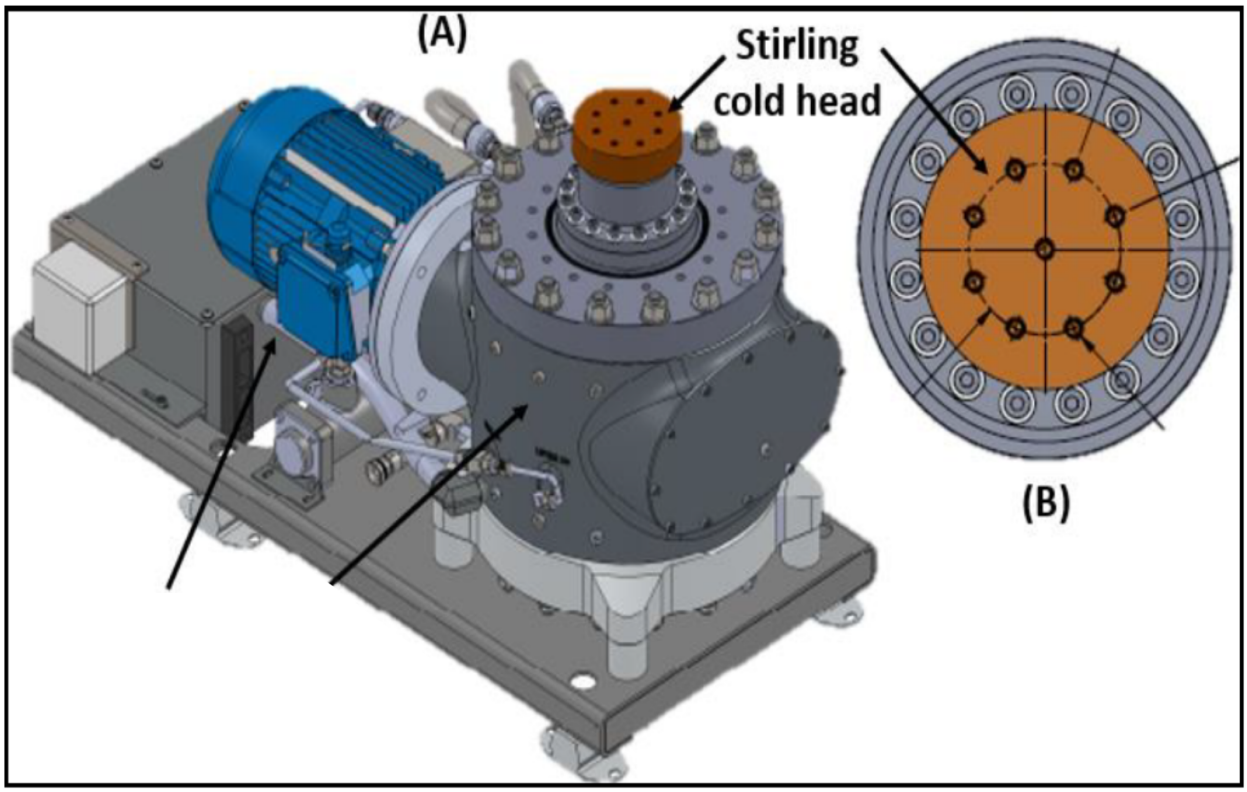

Figure 3.1.2. (A) Design of the AFCryo STC90 Cryocooler and Stirling Cold Head and (B) Overhead View of Stirling Cold Head (Meier et al., 2018)

The carbon dioxide is collected and stored on the cold head surface in the solid state at -159.07 ℉ in order to allow a significant amount of carbon dioxide to freeze and to ensure that the carbon dioxide stays well below its vapor pressure when frozen (Meier et al., 2018). The unit will use electricity from the generators to cool and freeze the carbon dioxide at this temperature. Based on Aspen calculations, the pressure of the gas at this temperature is 4.21 psi and it removes 11.92 kW of heat to cool the gas to this temperature. In order to solidify the gas at this temperature, the heat of sublimation is 26.3 kJ/mol, so -787.53 W of heat is needed to freeze all of our carbon dioxide gas at -159.07 ℉, also powered by electricity from the generators (Stull, 1947). At this temperature and pressure, argon and nitrogen remain in the gaseous state. At this point, a vacuum

pump pumps out the remaining gases. After this, the carbon dioxide is heated up with 8 cartridge heaters per unit and pressurized into a vapor at -128.24 ℉ and 13.7 psia. This requires a total of 787.53 W to sublimate the carbon dioxide. To pressurize and heat up the gas to the operating conditions above, a total of 10.81 W of heat should be added. Electricity from the generators will be used as power for these operations. Once these operating conditions are met, the heaters turn off and the carbon dioxide is sent to our carbon dioxide storage tank to meet up with the recycle stream. After this, the process begins again by fanning in more material from the atmosphere (Meier et al., 2018).

3.2 Desalination

The desalination system is composed of four distinct units, those being two heat exchangers, a vertical flash, and a pump. The consumption of each of the aforementioned units, as represented by duty values, is observable in the Aspen model shown in Figure 3.2.1. Specifically, physical characteristics related to dimensions and mass of the two heat exchangers and the pump are discussed in section 3.7 and section 3.9, respectively.

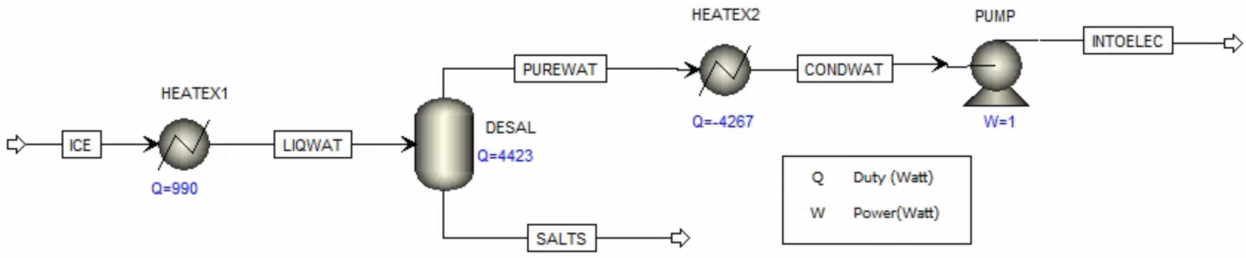

Figure 3.2.1. Aspen Model of Desalination System with Duty Values

In particular, the Martian ice is fed into the first heat exchanger at -76 ^{o}F and 13.7 psia. It entirely exists in the solid phase and includes impurities in the form of the following salts: magnesium sulfate, sodium sulfate, magnesium carbonate, calcium carbonate, and sodium chloride. The total mass flow rate of the Martian ice stream is 18.91 lb/hr. The mass flow rates of the individual components within the Martian ice stream correspond to the assumed composition of the liquefied Martian water mixture that is reflected in Table 2.4.1. The first heat exchanger operates at 154.4 ^{o}F and 13.7 psia and requires 990.2 W to conduct heating. The temperature of the first heat exchanger causes the Martian ice to melt, consequently exiting as liquid water at 154.4 ^{o}F and 13.7 psia. In reality, this stream is 92.46% liquid by mass and 7.54% solid by mass. Reactions will occur among the individual components within the liquefied Martian ice, thereby generating ionic species. The mass flow rates of the resultant components were determined using

the Electrolytes Wizard tool in Aspen coupled with the Elec-NRTL model, with the outcome contained in Table 3.2.1.

Table 3.2.1. Composition of Vertical Flash Inlet Stream

Component	Mass Percent
H_2O	82.50
Mg^{2+}	0.55
Ca^{2+}	0.14
Na^{+}	2.25
$MgCO_3$ (s)	4.61
$CaSO_4$ (s)	2.93
Cl^{-}	0.61
SO_4^{2-}	6.41
CO_3^{2-}	6.40×10^{-7}

This stream then enters a vertical flash at 13.7 psia that separates pure water from the salts, requiring 4,422.2 W to conduct heating. The pure water leaving the vertical flash is entirely in the vapor phase, with a temperature of 219.1 ^{o}F and a pressure of 13.7 psia. The total mass flow rate of the pure water stream is 13.03 lb/hr. Additionally, the vertical flash specifies a vapor fraction of 0.8 as the salts need not exit as dry products. Instead, the salts will be included in the remaining brine solution to be discarded. Just like the pure water stream, this brine solution has a temperature of 219.1 ^{o}F and a pressure of 13.7 psia. It is 74.28% liquid by mass and 25.72% solid by mass. Based on equations from Wankat (2012) for calculating the size of a vertical flash drum, the vertical flash was found to have a diameter of 0.10 ft, which equals 1.2 in, and a height of 0.41 ft, which equals 4.9 in, from which the volume was calculated to be 0.0034 ft^3, which

equals 5.9 in^3. Nickel alloy serves as the material of construction for the vertical flash. Multiplying the volume by the density of nickel alloy, which is 0.32 lb/in^3, yields a mass of 1.87 lb for the vertical flash.

The second heat exchanger then condenses the pure water leaving the vertical flash that is entirely in the vapor phase. The second heat exchanger operates at 72.5 ^oF and 13.7 psia and requires 4,266.7 W to conduct cooling. The effluent has a temperature of 72.5 ^oF and a pressure of 13.7 psia and entirely exists in the liquid phase. The necessity of the second heat exchanger is derived from the fact that purified liquid water at roughly 72.5 ^oF is required for the inlet stream of the electrolyzer. As the specifications of the electrolyzer also stipulate that the inlet stream be at 51.7 psia, a pump raises the pressure of the purified liquid water from 13.7 psia. The pump causes a slight temperature increase such that the inlet stream of the electrolyzer ultimately has a temperature of 72.8 ^oF and a pressure of 51.7 psia.

3.3 Electrolyzer

In determining the design of the electrolyzer, the first consideration involved selecting which type of hydrogen production technology would be most appropriate for our application. An analysis of the alkaline water and the proton exchange membrane (PEM) varieties was conducted (Guo et al., 2019). Advantages of alkaline water electrolyzers include that the technology is mature, manufacturing costs are low, and they are suitable for large-scale hydrogen production stations. However, alkaline water electrolyzers are disadvantageous in that start-up is slow, they are susceptible to corrosion, maintenance is complicated, and there are many components within a single unit. In contrast, advantages of PEM electrolyzers include that start-up is fast, they are not susceptible to corrosion, maintenance is simple, and there are fewer components within a single unit than in the case of alkaline water electrolyzers. However, PEM electrolyzers are disadvantageous in that manufacturing costs are high. Ultimately, PEM was chosen for the hydrogen production technology because maintaining structural integrity is of the utmost importance in the context of Mars due to the limitations related to upkeep caused by isolation from Earth. In particular, structural integrity is supported by the following benefits of PEM electrolyzers: they are not susceptible to corrosion, maintenance is simple, and there are fewer components within a single unit than in the case of alkaline water electrolyzers.

Specifically, the electrolyzer is based on the Nel C10 PEM Hydrogen Generation System, as depicted in Figure 3.3.1 (*Nel C Series*, 2021). The reaction is shown below as:

$$2H_2O \rightarrow 2H_2 + O_2$$

Figure 3.3.1. Nel C10 PEM Hydrogen Generation System

This particular system within Nel's C Series was selected for the electrolyzer because it produces hydrogen at a nominal rate of 10 Nm^3/hr. As the material balance in Figure 3.3.2 stipulates that 1.46 lb/hr of hydrogen exits the electrolyzer, which equals 0.66 kg/hr of hydrogen, the density of hydrogen can be used to convert this quantity into the unit of Nm^3/hr. The density of hydrogen vapor is 0.08375 kg/m^3 (*Basic Hydrogen,* n.d.), yielding a nominal hydrogen production rate of 7.9 m^3/hr, which is just below 10 Nm^3/hr at 0 ^oC and 1 bar. Per the operating conditions of the Nel C10 PEM Hydrogen Generation System, the electrolyzer has the following additional properties: a nominal delivery pressure of 435.1 psia, a power consumption of 6.2 kWh/Nm^3 of hydrogen, and a hydrogen purity of 99.9998%. The deionized water that is fed into the system has a consumption rate of 9 L/hr at maximum hydrogen production, a temperature of roughly 72.5 ^oF, and a pressure of 2.55 barg, which equals 51.7 psia.

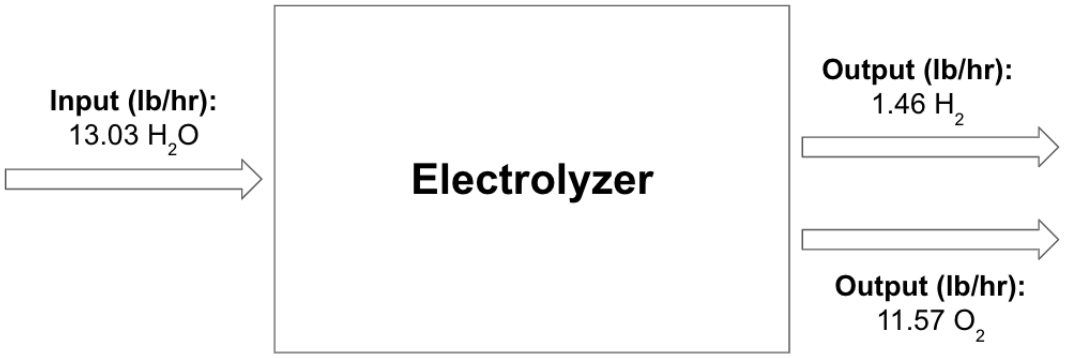

Figure 3.3.2. Material Balance for the Electrolyzer

In terms of the physical characteristics of the electrolyzer, the system is composed of two connected enclosures. That for the electrolyzer itself, which is depicted on the left side of Figure 3.3.1, has dimensions of 99” x 46” x 79”, while that for the power supply, which is depicted on the right side of Figure 3.3.1, has dimensions of 67” x 41” x 79”. The total weight is 6,027 lb.

Given the aforementioned design specifications, the efficiency of the electrolyzer can be calculated. The theoretical consumption of the unit is equivalent to the heat of formation of water, which has a value of -285.83 kJ/mol (*Water*, 2021). The actual consumption of the unit is derived from the power consumption, which was previously defined as 6.2 kWh/Nm^3 of hydrogen and can also be represented as 68.9 kWh/kg. Using the molecular weight of hydrogen and the mole ratio between water and hydrogen from the chemical equation for electrolysis, the actual consumption of the unit is found to be 499.97 kJ/mol. Since the magnitude of the theoretical consumption is less than that of the actual consumption, the efficiency is computed by dividing the former quantity by the latter quantity. In essence, this phenomenon demonstrates that the electrical capacity of the electrolyzer exceeds the electrical requirement of the reaction. The efficiency of the electrolyzer is 57.17%, as demonstrated by the calculations in Figure A.1 in Appendix A.

3.4 Sabatier Reactor

The design of the Sabatier reactor is based on the American Institute of Aeronautics and Astronautics (AIAA) design of a lab-scale Sabatier reactor (Junaedi et al., 2011). The reaction is shown below as:

$$CO_2 + 4H_2 \leftrightarrow CH_4 + 2H_2O$$

The kinetics of the reaction suggest the formation of solid carbon as a potential byproduct. To remedy this, the reaction occurs over a 0.5 wt% ruthenium on alumina catalyst, yielding methane selectivities of nearly 100% and eliminating any significant formation of solid carbon (Vogt et al., 2019). This catalyst was more expensive than commonly used nickel-based catalysts, but the increased durability and easier maintenance justified the decision to use ruthenium, since liftoff costs and astronaut labor far outweigh the cost of the material (Moioli & Züttel, 2020).

Due to the highly exothermic nature of the reaction, the reaction was designed to occur within a shell and tube heat exchanger, acting as the hot side of the exchanger. Liquid carbon dioxide acts as the cold side of the heat exchanger, which is captured by the atmospheric capture system and compressed to a pressure of 145 psi. Heat and mass transfer calculations were performed to maintain the methane selectivity and reactor efficiency, resulting in the tube sizings shown in Figure 3.4.1 below.

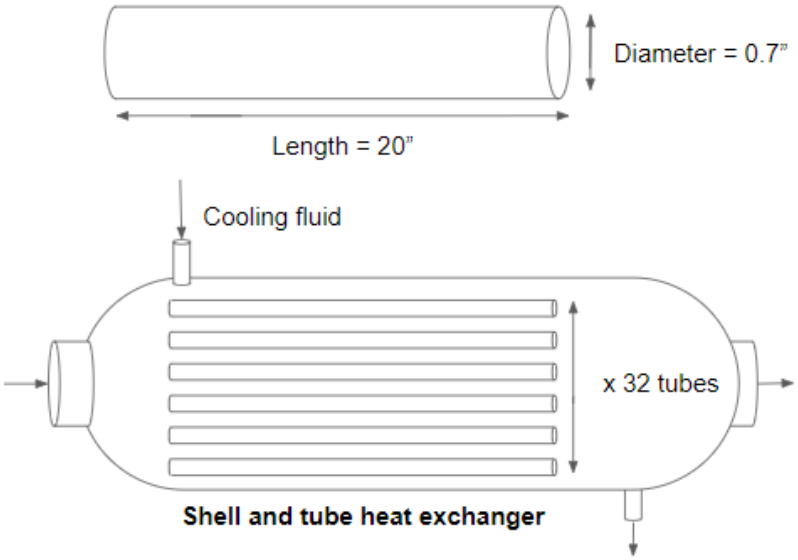

Figure 3.4.1. Design Schematic of the Sabatier Reactor

The material balance for the Sabatier reactor, which is represented by Figure 3.4.2, focuses on producing methane from hydrogen and carbon dioxide. It must produce 2.89 lb/hr of methane in order to produce enough fuel for a return trip to Earth. Including the recycled methane, the production of 3.69 lb/hr of methane is appropriate for this objective. The expected conversion rate for the reactor is 76% (Junaedi et al., 2011). Material balance calculations were performed based on these data points, and feed flow rates were found to be 10.44 lb/hr of carbon dioxide and 2.11 lb/hr of hydrogen.

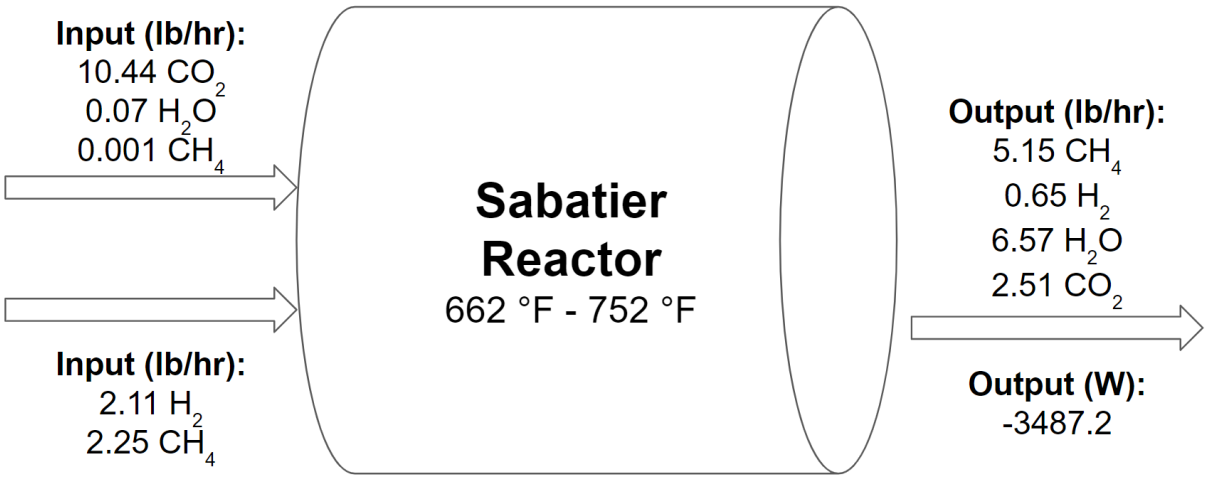

Figure 3.4.2. Material Balance Diagram for the Sabatier Reactor

In order to determine the pressure drop across the Sabatier reactor, the Reynolds number for a single tube in our packed bed reactor was calculated using an effective particle diameter of 0.13 inches (*Product Specification*, n.d). Porosity was determined from the volume of catalyst in each pipe. Based on this Reynolds number, the Ergun equation was used to determine the friction factor for a pipe in our reactor. Using this friction factor, the pressure drop was determined to be 3.90×10^{-4} psia, with calculations shown in Figure A.2 in Appendix A. This value is not significant compared to the reactor's operating pressure of 13.7 psia. This pressure was chosen because it was used in the experiments conducted by Junaedi et al. that serve as the basis for the reactor design. This is due to the low feed linear velocity. A heating jacket is required to heat up the carbon dioxide and hydrogen fed into the reactor to 662 °F. Due to the highly exothermic reaction, it would not be feasible to make the reactor isothermal or adiabatic, so it was decided that the reactor effluent would heat up to 752 °F to reduce the cooling demands, as this temperature should have little effect on the products of the reactor. This requires that 3,487.2 W of heat be removed.

Due to the large amounts of heat generated in the Sabatier reaction, the heat transfer design and calculations took precedence as the top priority. Liquid carbon dioxide was chosen as the cooling fluid due to its availability on Mars and the working range of its phases. Modeling the reactor as a shell and tube heat exchanger, the required heat transfer area was calculated using the Reynolds number, Prandtl number, and Nusselt number of both the reactor effluent and cooling fluid with Equation 3.4.3 and Equation 3.4.4. Equation 3.4.3 calculates the heat transfer resistance coefficient and Equation 3.4.4 calculates the area needed. The vaporization of liquid carbon dioxide was found to require 9.36 ft^2 of area for heat transfer, with 130.9 lb/hr of liquid carbon dioxide at 145 psia being used to remove the excess heat from the reactor.

Equation 3.4.1 $h_i = \frac{Nu*k}{D_i}$

Equation 3.4.2 $h_o = \frac{Nu*k}{D_H}$

Equation 3.4.3 $U_o = [\frac{1}{h_o} + \frac{r_o \ln(\frac{r_o}{r_i})}{k} + \frac{r_o}{h_i * r_i}]^{-1}$

Equation 3.4.4 $A = \frac{U_o \Delta T_{lm}}{Q}$

The packed bed reactors are composed of stainless steel tubing, per the lab-scale reactor design that served as the basis for our own design (Junaedi et al., 2011). The catalyst materials used for the construction of our reactor have been performance tested in environments that simulate the conditions involved with sending the reactors to Mars and operating them there (Franco et al., 2019). One study contrasted baseline reactors and test cases that examined the effects of vibration, liquid water exposure, and particle and chemical contamination (Franco et al., 2019). This study ultimately found that all of the catalysts performed well and did not deviate significantly in terms of methane production over a period of 120 hours (Franco et al., 2019).

This suggests that our catalysts would be effective for the chosen time frame. Furthermore, the selectivity to produce methane of the selected catalyst did not decrease over about 100 hours in the study that served as the basis for our design (Junaedi et al., 2011).

The Sabatier reactor and subsequent units are observable in the Aspen model shown in Figure 3.4.3.

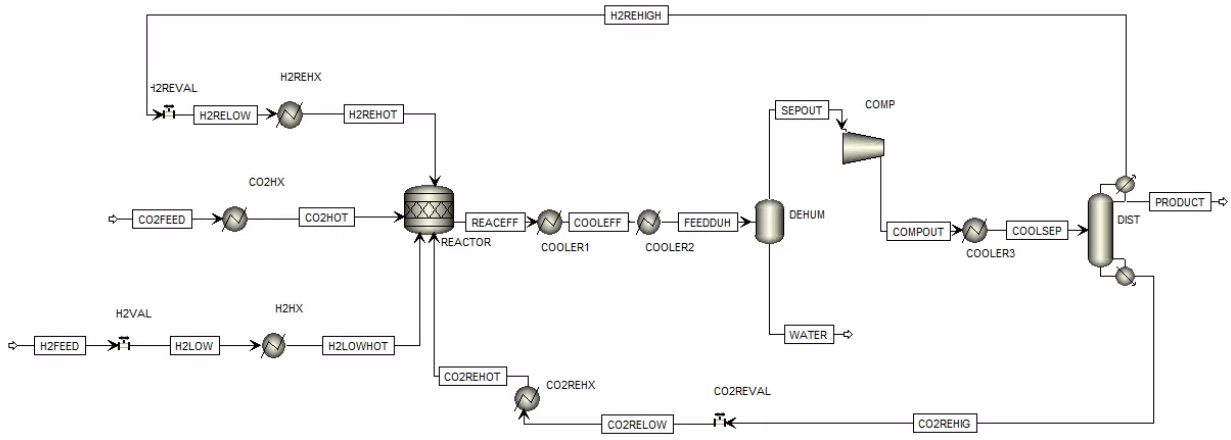

Figure 3.4.3. Aspen Model of Sabatier Reactor and Subsequent Units

3.5 Dehumidifier System

The dehumidifier system is composed of two sections. The first section is the coolers. Cooler 1 is arranged between the reactor and Cooler 2, and its purpose is to cool the reactor effluent stream to its dew point temperature, which aids in the removal of water. Due to the high temperatures generated by the exothermic Sabatier reaction, Cooler 2 was designed to cool the reactor effluent from the dew point temperature to a temperature at which the separation of water would occur at higher yields. These coolers are discussed in further detail in section 3.7. The second section is the dehumidifier. The dehumidifier was designed as a flash drum to separate the liquid water from the remaining reactor effluent vapors. This separation is especially important because the formation of ice in the product would present safety issues and product impurities.

Flash Drum Design

The flash drum was designed to remove water from the product stream before having it undergo the final separation step. The flash was simulated in Aspen and yielded 99.3 mass percent separation of water from the product stream. Flash drum design calculation procedures from *Separation Process Engineering* were employed to determine the necessary sizing of the dehumidifier (Wankat, 2007). The results of these calculations are listed in Table 3.5.1 below.

Table 3.5.1. Dehumidifier Sizing Results

Dimension	Size
Area	0.18859 ft^2
Diameter	0.49002 ft
Height	1.9601 ft
Volume	0.36964 ft^3

3.6 Product Separation

The final separation block aims to separate methane from the rest of the reactor effluent, specifically trace amounts of water, carbon dioxide, and hydrogen. This is achieved by cryogenic distillation and the separation of methane from hydrogen through liquefying methane while hydrogen stays in the vapor phase. The temperature range for carbon dioxide and methane condensing temperatures are -40 ^{o}F and -191.2 ^{o}F at 145 psi. However, as hydrogen makes up a large portion of the final product separation by mole, the required temperature to condense methane is around -238 ^{o}F.

To counteract the lower temperatures required to condense methane as the ratio of hydrogen to methane in the product stream increases with lower vapor fractions coming out of the distillation column, not all of the methane will be condensed. This non-liquefied methane and hydrogen is recycled to the reactor, increasing the overall efficiency conversion of the reactor to 99%. While some methane is recycled, it makes up about 10% of the recycle stream by mole, and the recycle stream constitutes about 10% of the overall feed to the reactor. This 1% of recycled methane has little effect on the efficiency of the equilibrium reaction, but demands a higher duty on all the processes in the rocket fuel plant.

These low condensing temperatures are achieved by using liquid nitrogen at higher pressures to cool the products in the condenser at the top of the distillation column, including the reflux stream. Roughly 13.2 lb/hr of liquid nitrogen is required to cool the distillation column's condenser and material flowing through it. Liquid nitrogen is produced by a Creare ACS system, which is discussed further in section 3.8. The temperature of this liquid nitrogen is -320.8 ^{o}F. This column has 6 stages, including the condenser and the reboiler, with a diameter of 0.089 ft and a height of 8 ft. The condenser has a duty of -1,515 W and the reboiler has a duty of 940 W.

These duties are achieved using liquid nitrogen and electric heaters, respectively. The column also has a reflux ratio of 2 in terms of moles and a distillate vapor fraction of 0.5. This was modeled in Aspen, through which all of the column internals were determined.

As some assumptions had to be made about the electrolyzer selected for the process, we assumed the same conditions for the oxygen stream as the hydrogen stream. These assumptions include a practically pure stream of oxygen, an outlet pressure of 435.1 psi, and an outlet temperature of 69.8 ^{o}F. This stream is also liquefied using liquid nitrogen as a cooling fluid, which is accomplished by reducing the pressure to 145 psi and a temperature of -245.5 ^{o}F.

3.7 Heat Exchangers

In order to determine the dimensions of the heat exchangers, Equation 3.7.1 was utilized (Carta, 2021). In this equation, Q denotes the heat transfer rate or duty, U denotes the overall heat transfer coefficient, A denotes the cross-sectional area of the inner tube perpendicular to the heat transfer flux, and ΔT_{lm} denotes the logarithmic mean temperature difference between the hot and cold streams.

Equation 3.7.1. $Q = UA\Delta T_{lm}$

For each heat exchanger in the process, the value of Q was generated by Aspen, the value of U was selected from an assemblage of possible estimations in the heat exchanger design heuristics document based on the phases involved (Peters et al., 2003), and the value of ΔT_{lm} was calculated from known stream temperatures, thereby allowing for the value of A to be solved for. The outer tube area, the inner tube diameter, the outer tube diameter, the tube length, the mass of the heat exchanger, and the required mass flow of coolant were computed from the inner tube area. In particular, liquid carbon dioxide at -40 ^{o}F and 145 psia was selected as the coolant.

As aforementioned, two of the distinct units in the desalination system depicted in Figure 3.2.1 are heat exchangers. The first heat exchanger functions as a heater for the purpose of melting the Martian ice such that it exits the heater as liquid water with solid impurities in the form of salts and ionic species generated by the individual components within the liquefied Martian ice. This heating requires a duty of 990.2 W. In terms of the value of U, the phase change at hand most closely corresponds to a heat transfer coefficient of 285 W/m^2-K, which typically represents liquid to liquid transitions. As the inlet stream temperature is -76 ^{o}F and the outlet stream temperature is 68 ^{o}F, 116.33 ^{o}F was decided upon for the heat source temperature,

which was supplied through heating jackets powered by electricity, as it represents a sufficient value for driving heat transfer. The inner and outer tube areas are 0.52 ft^2, which equals 74.9 in^2, and 0.77 ft^2, which equals 110.9 in^2, respectively. Therefore, the inner and outer tube diameters are 0.11 ft, which equals 1.3 in, and 0.15 ft, which equals 1.8 in, respectively. The tube length is 0.66 ft and the mass of the heat exchanger is 1.86 lb.

The second heat exchanger in the desalination system functions as a cooler for the purpose of condensing the pure water vapor leaving the vertical flash such that it exits the cooler as purified liquid water. This cooling requires a duty of 4,266.7 W. In terms of the valve of U, the phase change at hand most closely corresponds to a heat transfer coefficient of 850 W/m^2-K, which typically represents transitions across condensers. As the inlet stream temperature is 219.08 ^oF and the outlet stream temperature is 72.5 ^oF, 44.33 ^oF was decided upon for the coolant temperature as it represents a sufficient value for driving heat transfer. The inner and outer tube areas are 0.55 ft^2, which equals 79.2 in^2, and 1.63 ft^2, which equals 234.7 in^2, respectively. Therefore, the inner and outer tube diameters are 0.11 ft, which equals 1.3 in, and 0.28 ft, which equals 3.36 in, respectively. The tube length is 0.66 ft, the mass of the heat exchanger is 3.85 lb, and the required mass flow of coolant is 103.72 lb/hr.

The heat exchangers used in the dehumidifier system were designed as double pipe heat exchangers. Due to the low flow rates produced in the reactor effluent, multiple passes were determined to be unnecessary for the required cooling. The Aspen simulation of Cooler 1 showed that this unit cools the reactor effluent from 752 ℉ to the dew point temperature of 177.71℉, netting a heat duty of -1,156.4W. Aspen was also used to simulate Cooler 2, which was designed to cool the effluent from Cooler 1 to a temperature of 35.6 ℉. This was done to perform the final liquefication of water from the otherwise vapor stream, netting a heat duty of -2,390 W.

Liquid carbon dioxide at a feed temperature of -40 °F was used as the coolant for these exchangers. The heat exchanger design heuristics document from Peters et al. (2003) was used to determine the dimensions of the coolers. Using a value of 30 W/m^2-K from Peters et al. (2003), it was determined that Coolers #1 and #2 require a heat transfer area of 5.2057 ft^2 and 17.6411 ft^2, respectively.

Cooler 3 comes after a compressor and is meant to reduce the temperature of the product stream before the distillation column in order to reduce overall power consumption and ensure an easier separation of products. It cools the product stream from 544 ^{o}F down to 22 ^{o}F and has a cooling duty of 4,266 W, taken from the Aspen model. This heat exchanger, like Coolers #1 and #2, is also cooled with liquid carbon dioxide at -40 ^{o}F. Using the appropriate U value from the heat exchanger design heuristics document (Peters et al., 2003), a heat transfer area of 4.06 ft^2 was required. This caused the design to be a double pipe heat exchanger that is 1 ft long and has diameters of 0.447 ft and 0.468 ft for inner and outer pipes, respectively. The overall mass for this heat exchanger is 10.06 lb.

The carbon dioxide streams require two heat exchangers, one after the atmosphere separator and another on the recycle stream coming from the bottom of the distillation column. The purpose of these heat exchangers is to raise the temperature of the feed streams to the reactor to the desired activation temperature of 662 ^{o}F. The temperatures of these streams before their heat exchangers is -128.2 ^{o}F and -38.5 ^{o}F, respectively. The stream from the atmosphere separator has a duty of 409.5 W and the recycle stream has a duty of 248.1 W. A U value of 30 W/m ^{2}-K from Peters et al. (2003) was used for area calculations as the internal materials are in the gas phase. Heating energy is supplied through heating jackets powered by electricity on the outside of the pipes at a temperature of 751 ^{o}F. The required heat transfer areas are 0.76 ft^2 and 0.5 ft^2

with pipe lengths of 1 ft and 0.5 ft, respectively. This causes their pipe diameters to be 0.11 ft and 0.12 ft with masses of 2.11 lb and 1.675 lb.

The hydrogen streams follow the same heat exchanger requirements as the carbon dioxide streams. One is required after the electrolyzer and another exists on the recycle stream coming from the top of the distillation column. The temperatures of these streams before their heat exchangers are 70.8 ^{o}F and -243.7 ^{o}F, respectively. The stream from the electrolyzer has a duty of 874.0 W and the recycle stream has a duty of 950.2 W. A U value of 30 W/m ^{2}-K from Peters et al. (2003) was used for area calculations as the internal materials are in the gas phase. Heat energy is supplied through heating jackets powered by electricity on the outside of the pipes at a temperature of 751 ^{o}F. The required heat transfer areas are 1.9 ft^2 and 1.6 ft^2, respectively, with both pipe lengths being 2 ft. This causes their pipe diameters to be 0.11 ft^2 and 0.12 ft^2 with masses of 3.11 lb and 4.36 lb.

The oxygen coming out of the electrolyzer needs to be liquefied, and therefore cooled to a temperature of -245.5 ^{o}F. The oxygen comes in at 58.73 ^{o}F and is cooled using liquid nitrogen at -321 ^{o}F. Using a U value of 850 W/m^2-K from the heat exchanger design heuristics document as this is a condensing heat exchanger (Peters et al., 2003), it was found that the heat transfer area required was 0.151 ft^2. Since the heat transfer area is small, this heat exchanger was modeled as a double pipe heat exchanger with a length of 0.25 ft and diameters of 0.021 ft and 0.191 ft for inner and outer diameters, respectively. The overall mass of this heat exchanger came out to 1.40 lb. The oxygen condensing stream with its heat exchanger is observable in the Aspen model shown in Figure 3.7.1.

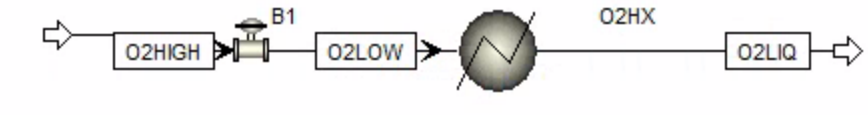

Figure 3.7.1. Aspen Model of Oxygen Condensing Stream

The distillation column has two heat exchangers, a condenser, and a reboiler. The condenser cools the top products of the distillation column while also condensing some of the top output for product storage. It operates at -234.7 ^{o}F and has a duty of 1.515 kW. Using a U value of 850 W/m^2-K as it is a condenser (Peters et al., 2003), the area for heat transfer was determined to be 0.037 ft^2 when cooled with liquid nitrogen at -321 ^{o}F. As the heat transfer area is small, a double pipe heat exchanger was selected with an inner and outer diameter of 0.022 ft and 0.394 ft, respectively. The length came out to 0.3 ft with an overall mass of 3.87 lb.

The purpose of the reboiler is to ensure acceptable separations from the distillation column. It was decided that a heating jacket on a pipe would suffice as a reboiler as long as some entrainment occurs at the bottom. This reboiler operates at a temperature of 67.73 ^{o}F and has a duty of 950 W. Its required heat transfer area is 0.16 ft^2 using a U value of 1,100 W/m^2-K from the heat exchanger design heuristics document (Peters et al., 2003), resulting in a bottoms stream at -38.5 ^{o}F. This causes a pipe diameter of 0.046 ft and length of 0.5 ft. The overall mass of the reboiler is 1.244 lb.

3.8 Liquid Nitrogen Recycle System

Liquid nitrogen is utilized to liquefy both final product streams of methane and oxygen. Liquid nitrogen was chosen as its temperature is lower than that of both product streams, would have good heat transfer properties, and could be reasonably produced on Mars. Our process uses liquid nitrogen at 14.7 psi and -321 ^{o}F, assuming that all the heat transferred vaporizes this stream rather than changing its temperature (Plachta et al., 2017). The system recycles the vaporized nitrogen, therefore requiring only a small amount of nitrogen to be sent from the Earth. As there is a lack of available literature to instruct the design of our own system with reasonable power consumption, we opted to select one designed and funded by NASA.

Selected System

The system selected is the Creare ACS cryocooler unit. This design has a mass of 33 lb and an output of 20 W worth of cooling. For every 1 W of cooling power, it requires an input of 15 W of electrical power (Plachta et al., 2017). This can be scaled up directly to supply our liquid nitrogen demand for liquefying our product streams. Any rejected heat can be sent to the rest of the Mars operational units rather than the atmosphere or regolith, but that was determined to be out of the scope of this project.

Sizing and Scaling

Liquid nitrogen is only used in the distillation condenser and oxygen heat exchanger as there are no other reasonable options for cooling in these processes. Overall, we wanted to limit the usage of liquid nitrogen as it is economically intensive to employ on Mars. The liquid nitrogen requirements for each unit are given in Table 3.8.1 These calculations assume complete vaporization of the liquid nitrogen, thereby allowing maximum usage of it. As the heat capacity of nitrogen is small, it would require much more heat transfer area if the vaporized nitrogen was

also used to cool the process. The calculations related to these demands are covered in more detail in section 3.7.

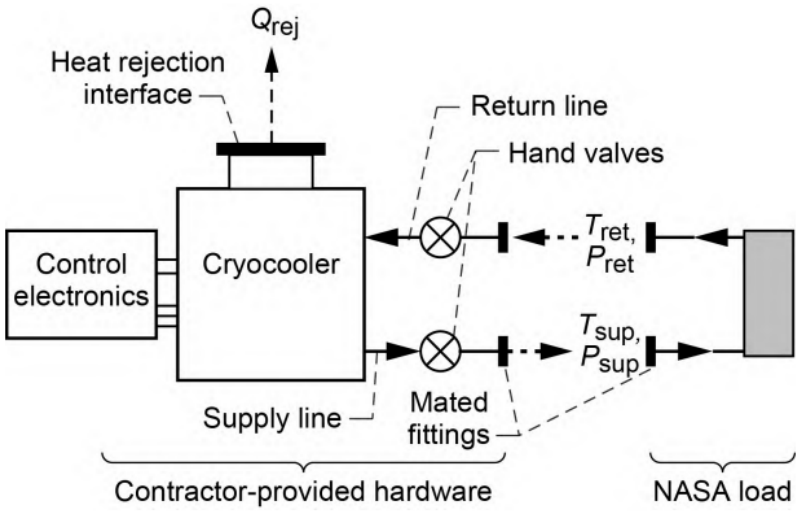

Figure 3.8.1 Schematic of the Creare Cryocooler Unit

The Creare unit was scaled for the 2,017 W cooling demand based on 20 W of cooling per 33 lb. The electrical power requirements were scaled with the heat duty based on 15 W per 1 W of cooling, which resulted in a power requirement of 30.255 kWe for the unit. The total mass of liquid nitrogen to be sent is 80.35 lb to allow for an hour's worth of material in the process.

Table 3.8.1. LN_2 Requirements for Cryogenic Cooling

Unit	Heat Duty (W)	Electrical Duty (W)	LN_2 Flow Rate (lb/hr)
Distillation Condenser	1,515	22,725	60.35
O_2 Condenser	502	7,530	20.00
Total Demand	2,017	30,255	80.35

3.9 Pumps and Compressors

As aforementioned, one of the distinct units in the desalination system is a pump. The purpose of this pump is to raise the pressure of the resultant purified liquid water before entering the electrolyzer. Specifically, the design of the pump is based on the United States Plastic Corp. Medium/High Flow Variable Speed Pump, as depicted in Figure 3.9.1 (*Medium/High Flow*, n.d.). It has a mass of 2.9 lb and a unit price of $916.37, which will be accounted for in the upcoming economic analysis.

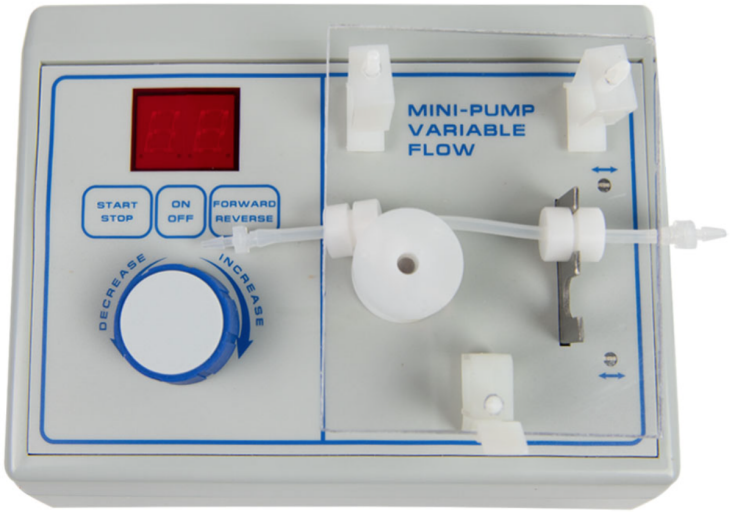

Figure 3.9.1. United States Plastic Corp. Medium/High Flow Variable Speed Pump

This particular system was selected as the basis for the design of the pump because it handles fluid traveling between 4.0 mL/min and 600 mL/min. In reality, the volumetric flow rate of the purified liquid water traversing the water pump is 98.7 mL/min, a relatively low value which falls within the acceptable range for this piece of equipment and indicates the suitability of a lab-scale peristaltic variation such as the United States Plastic Corp. Medium/High Flow Variable Speed Pump. The volumetric flow rate was obtained through modeling in Aspen, as were the additional properties of fluid power, which is 0.431 W, and pressure change, which is

37.9802 psia. Separately, the mass flow rate of this purified liquid water is 13.0299 lb/hr. It was later determined that pumps are required for product streams. This pump is also suitable for these streams as the flow rates are similarly small. Using Aspen the flow rates were calculated to be 55 mL/min of methane and 91.1 mL/min of oxygen. No pressure change is required for these streams.

As the final products need to be pressurized to liquefy, a compressor is utilized to increase the reactor effluent after dehumidifying to a pressure of 145 psi and before being sent to the cryogenic distillation column. This reactor effluent stream consists of methane, carbon dioxide, hydrogen, and trace amounts of water. The compressor chosen for this task was a two stage Ingersoll Rand air compressor rated for 5 horsepower, as seen below in Figure 3.9.2. It costs $1,812.31 and weighs 425 lb.

Figure 3.9.2. Ingersoll Rand Electric Air Compressor (*Electric Air Compressor, n.d.)*

This compressor was chosen as it exceeds the required operating capabilities of our system. While the horsepower output is up to 5, it only needs to operate at 1.5 horsepower, which was determined through modeling in Aspen. Horsepower was used for defining this piece of equipment as this unit of measurement serves as the typical means of communication for the power ratings of compressors. For the process pressures, this compressor can handle operating pressures up to 175 psi, but it does not need to exceed 145 psi. This compressor can also run at 100% continuous duty, which will be required as our process is supposed to run 24 hours a day and 7 days a week (*Electric Air Compressor*, n.d.).

3.10 CO_2 Heat Dump

As the Sabatier reactor produces significant amounts of heat and our product is required to be at cryogenic temperatures, our process is designed by leveraging the cold temperatures of Mars to act as a heat dump for our system. Mars is, on average, -76 ℉ with winds of around 6.4 ft/s. All of our cooling that does not utilize liquid nitrogen was designed to be cooled by liquid carbon dioxide at -40 ℉ and 145 psi, where all of the heat absorbed was modeled as vaporizing the fluid. This was specified to reduce heat transfer areas and piping sizes as well as to simplify the system. Carbon dioxide was chosen as the coolant as it can be condensed from the atmosphere on Mars to reduce liftoff costs. After the coolant has been vaporized, it is recondensed through both convective heat transfer and radiative heat transfer. Combining the duties of all the cooling utilizing this carbon dioxide resulted in 13.199 kW and demand for 320.76 lb/hr of liquid carbon dioxide.

Convective heat transfer was modeled with the atmosphere of Mars at a temperature of -76 ℉, a constant wind speed of 6.4 ft/s, a pressure of 0.095 psi, and a composition of completely carbon dioxide. As the major heat transfer resistance derives from the conditions of the Martian atmosphere, it was only considered when calculating convective heat transfer. Convective heat transfer's contribution of energy dissipation was calculated using the heat transfer coefficient, h, which was determined from the equations below, where v is velocity, Q is the rate of heat transferred, A is the heat transfer area, D is the diameter of the pipe, ρ is the density, ΔT is the temperature difference, Cp is the heat capacity of the fluid, k is the thermal conductivity, Re is the Reynolds number, Pr is the Prandtl number, Prc is the corrected Prandtl number, Nu is the Nusselt number, and μ is the absolute viscosity (Gscheidle and Killian, 2017).

Equation 3.10.1. $\mathrm{Re} = \frac{vD\rho}{\mu}$

Equation 3.10.2. $\mathrm{Pr} = \frac{Cp\mu}{k}$

Equation 3.10.3. $\mathrm{Prc} = \left[1 + \left(\left(\frac{0.322}{Pr}\right)^{11/20}\right)^{-20/11}\right]$

Equation 3.10.4. $\mathrm{Nu}_{laminar} = 0.766[\mathrm{Re}*\mathrm{Prc}]^{1/6}$

Equation 3.10.5. $\mathrm{h} = \frac{kNu}{D}$

Equation 3.10.6. $Q = hA\Delta T$

Radiative heat transfer was also modeled to help reduce the amount of equipment being sent to Mars as the relatively thin atmosphere assists in increasing the efficiency of radiative heat transfer. Radiative heat transfer was modeled as having half of the area facing towards space and the other half facing towards the regolith of Mars. Radiative heat transfer's contribution of heat dissipation was modeled using the following equation, where ε is emissivity, σ is the Stefan-Boltzmann constant, T_{hot} is the temperature of the condensing carbon dioxide, T_r is the temperature of the regolith, and T_s is the temperature of space (Gscheidle and Killian, 2017).

Equation 3.10.7. $Q = \varepsilon\sigma A(0.5(T_{hot}^4 - T_r^4) + 0.5(T_{hot}^4 - T_s^4))$

The temperature of the internal fluid, space, and the regolith are -40 ℉, -76 ℉, and -454.8 ℉, respectively. Black paint was selected as a thin layer coating on the piping to increase emissivity to 0.95. Combining the two heat transfer rate equations and solving for the heat transfer area required gives the following equation:

Equation 3.10.8. $A = \frac{Q}{\varepsilon\sigma(0.5(T_{hot}^4 - T_r^4) + 0.5(T_{hot}^4 - T_s^4)) + \Delta Th}$

Using this equation gave a heat transfer area of 1,324 ft^2 in order to meet the cooling demands of the system. A diameter of 4 inches and a total of 100 pipes led to a length

requirement of 12.85 ft for each pipe. Combining the volume of all of the pipes and picking aluminum as the material led to an overall mass for this piece of equipment of 6,318 lb.

3.11 Tanks

The only tank deemed within the scope of this project is the carbon dioxide tank that takes in recovered carbon dioxide from the recycle stream as well as pure carbon dioxide from the atmospheric separation unit. The outlet stream of the tank is sent directly to the Sabatier reactor. The total inlet volumetric flow rate is 212.09 ft^3/hr, with 153.49 ft^3/hr coming from the purified CO_2 stream from the atmosphere and 53.60 ft^3/hr coming from the CO_2 recycle stream. These volumes are based on the fact that the materials are held at 662 ℉ and 13.7 psi to match the inlet flow conditions to the reactor. A 10-minute holding time was used for the CO_2 as this is considered a short-term storage unit. Multiplying the total volumetric flow rate by this time allowed for a determination of the total interior volume of the storage unit to be made, which is 35.35 ft^3. Based on the industry standard for normal cylindrical pressure vessels, the design uses a 1:1 ratio of diameter to length. Therefore, the inner diameter and the length are both 3.56 ft. The conditions for the tank sizing are displayed in Figure 3.11.1.

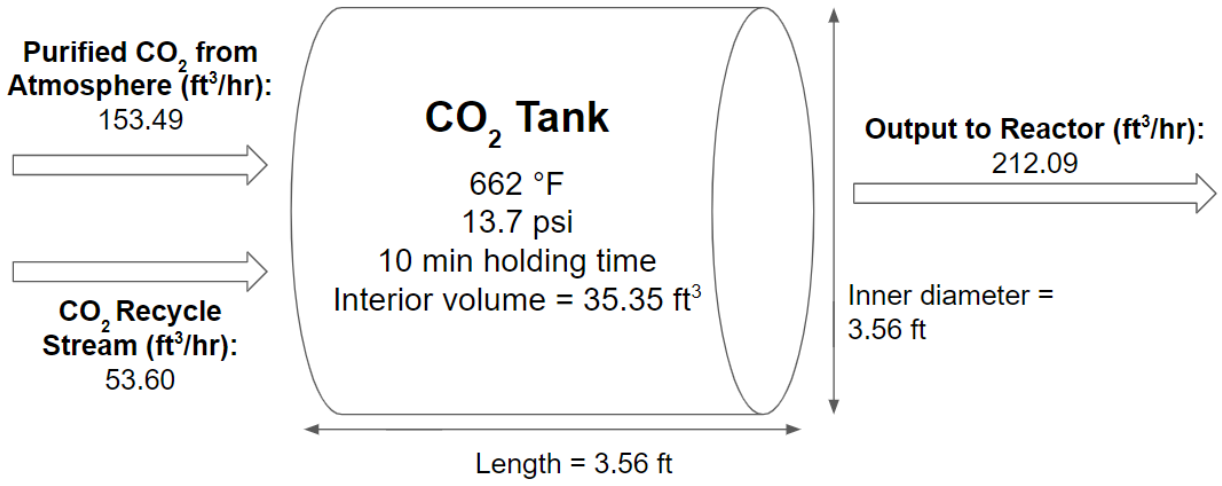

Figure 3.11.1. Summary of Design Parameters of CO_2 Tank

A stream table for the mass flow rates of the materials found in each of these streams is shown in Table 3.11.1.

Table 3.11.1. Inlet and Outlet Flow Rates for CO_2 Tank

Streams	Heated Pure CO_2 Feed	Heated CO_2 Recycle	CO_2 Feed
Temperature (℉)	662	662	662
Pressure (psi)	13.7	13.7	13.7
CO_2 (lb/hr)	7.94	2.50	10.44
H_2O (lb/hr)	0.00	0.07	0.07
CH_4 (lb/hr)	0.00	0.001	0.001

The tank is made of aluminum as it is compatible with the carbon dioxide being stored and it is stable at the temperatures and pressures that are used for the tanks. It is important to determine the weight of the aluminum for liftoff cost purposes. Using a form of Barlow's formula (Equation 3.11.1) allows for the thickness of the carbon dioxide tank to be computed, where t is the thickness, P is the pressure, d_i is the inner diameter, S is the surface area, E is the seam joint factor, and F is the design factor (Legal Information Institute, n.d.).

Equation 3.11.1. $$t = \frac{Pd_i}{2SEF - P}$$

The inner diameter is 3.56 ft, the yield strength of aluminum is 40,030 psi, the seam joint factor is unity because tanks are generally modeled as seamless, and the design factor is 0.72 (Thomasnet, n.d.; Legal Information Institute, n.d.). Using this formula, the thickness was calculated to be 0.01 inches. However, in order to improve heat transfer of the tank and ensure its stability at the low atmospheric temperatures of Mars, the tank was designed to have a thickness

of 0.39 inches. Based on this, the aluminum was calculated to be 222 lb due to a shell volume of 1.32 ft^3 (Density of Aluminum, n.d.).

The insulation for this tank is a 37-layer double aluminized mylar multilayer insulation (MLI) with a spunbond polyester spacer, based on a study quantifying its use for cryogenic applications (Ross, 2015; Multi Layer Insulation (MLI) Vacuum Insulation, n.d.). In order to determine the amount of insulation required to maintain the conditions required for the tank, the heat transfer formula shown in Equation 3.11.2 was used (Carta, 2020; Ross, 2015).

Equation 3.11.2. $$q = \frac{\Delta T^* SA}{\frac{n_L}{h} + \frac{t}{K}}$$

In this formula, q is the overall heat transfer in W and ΔT is the difference in temperature between the inside of the tank and the outside of the atmosphere, which is estimated as -63.67 ^oF, as explained in section 3.1. The surface area, SA, was calculated to be 59.72 ft^2. The number of layers of Mylar MLI, n_L, is 37 layers. The heat transfer coefficient for this insulation, h, is 0.025 W/m^2-K, and it was taken from the same study. The thickness of the aluminum shell is t, and K represents the thermal conductivity of aluminum, which was estimated to be 236 W/m-K at the given conditions (Carta, 2020). Using this formula, the required energy to insulate the tank is 1.21 W.

3.12 Power

Power for our system is provided through NASA's modular nuclear reactor known as Kilopower, which was designed to fill the gap for deep space energy requirements between 100 W class systems and 100 kWe class reactor power systems being developed for human exploration missions (NASA 2018). Kilopower reactors generate heat through fission at 1,562 ℉, which is then converted to electricity through Stirling engines utilizing molten sodium and a large titanium heat exchanger to generate a temperature gradient (Mason et al., 2013). It is worth noting that molten sodium can be dangerous because it reacts explosively with water, but the lack of water on Mars suggests that this is not a major cause for concern in our case. As the power comes from fission, the reactors are expected to reliably last for many years and to be capable of running at all times. In contrast, other options such as solar are characterized by inconsistent power generation.

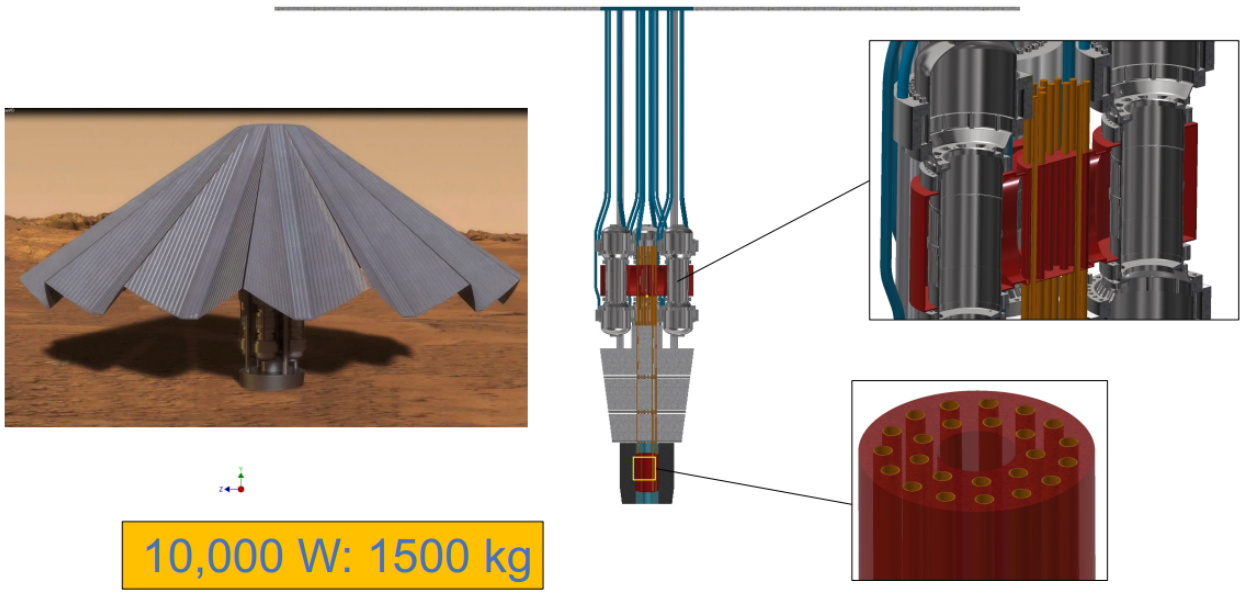

Figure 3.12.1 Kilopower Reactor Profiles (NASA, 2018)

Current testing on the Kilopower reactors running in adverse conditions have shown them to be resilient to changes in operating capacity and reactor temperature. Kilopower reactors can also handle changes in energy demand passively, therefore increasing the resiliency to the changing power consumption of the processes should something shut down or fail unexpectedly. NASA has also demonstrated that the reactors can be run passively for a class of reactor rated for 10 kWe. Because of these considerations, Kilopower reactors have been selected as the current power generation option. However, as NASA develops better designs, it is recommended that those be selected for future Mars missions.

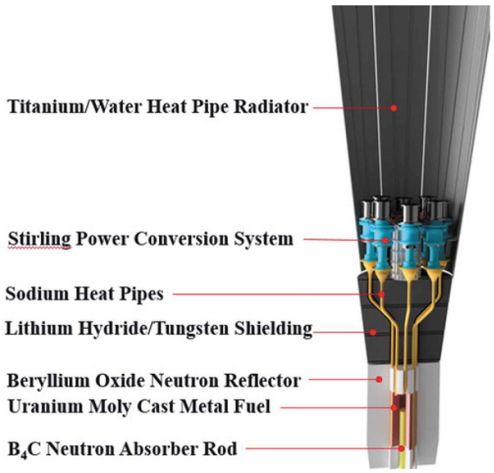

Figure 3.12.2 Kilopower Cut Away Profile (Mosher, 2018)

3.13 Excess Water Generation

The reaction that generates our rocket fuel produces water as a byproduct to methane. This water can be utilized elsewhere by the astronauts on Mars, thereby reducing the amount of potable water required to be shipped from Earth and consequently decreasing mission costs. The ISS loses about 2.26 lb of water per day on average through air locks and general cleaning even though its recovery system can recover 93% of used water (Allison, 2016). Our process produces 6.5 lb of water per hour, which is significantly more than that required by the ISS. This reality is capable of greatly impacting the savings associated with producing rocket fuel through in-situ resource utilization rather than shipping it to Mars. However, as there is a lot of uncertainty with regard to mission planning and demands, two primary economic scenarios will be analyzed in the upcoming economic sections. These include the case in which water generation is ignored and the case in which water is not assigned its own cost but it is instead accounted for in terms of liftoff cost savings.

4. Final Process Design

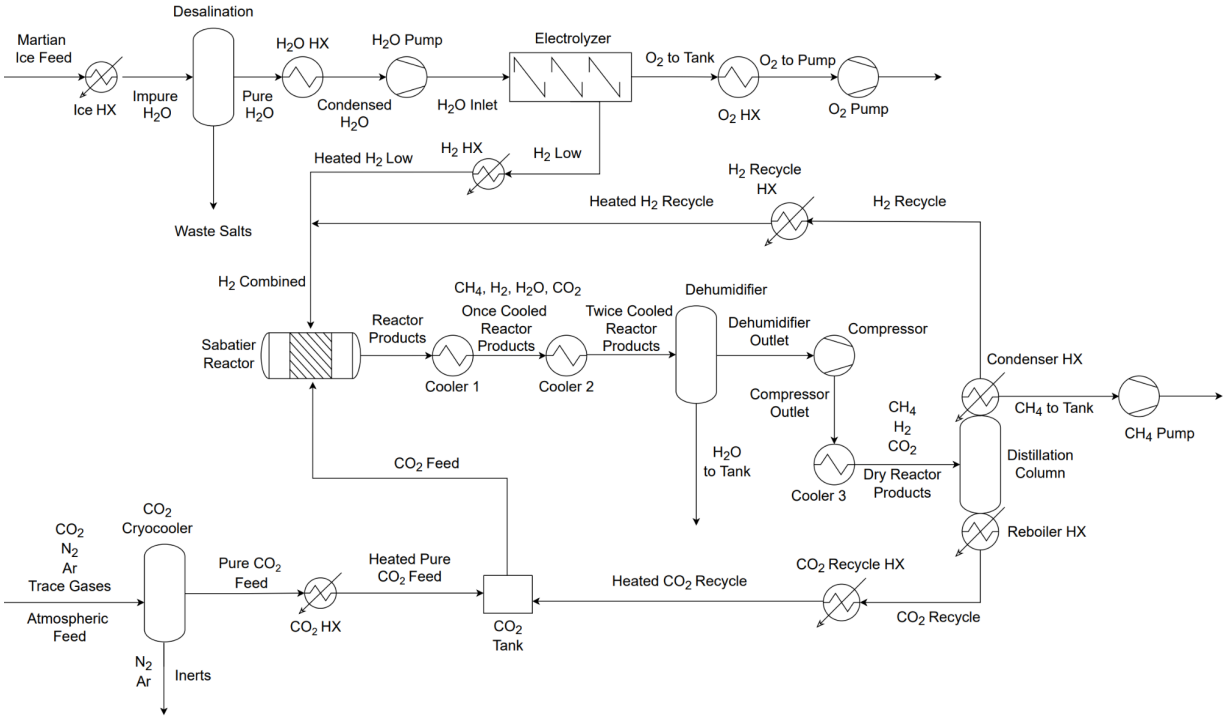

Figure 4.0.1 Full Process Flow Diagram with Stream Names for Mars ISRU Process

Table 4.0.1. Full Process Stream Table

Streams	Pure CO_2 Feed	Heated CO_2 Recycle	CO_2 Feed	H_2O Inlet	O_2 to Pump	H_2 Low	H_2 Recycle	H_2 Combined	Reactor Products	Dry Reactor Products	H_2O to Tank	CH_4 to Tank
Phase	Vapor	Vapor	Vapor	Liquid	Liquid	Vapor	Vapor	Vapor	Vapor	Vapor/ Liquid	Liquid	Liquid
Temperature (℉)	-128	662	662	72.7	-245	71	-243.7	71	752	-22	35.6	-234.8
Pressure (psi)	13.7	13.7	13.7	51.7	145	435.11	145	13.7	13.7	145	13.7	145
H_2 (lb/hr)	0	0	0	0	0	1.46	0.65	2.11	0.65	0.65	0	0
CO_2 (lb/hr)	7.94	2.50	10.44	0	0	0	0	0	2.51	2.51	0	0
H_2O (lb/hr)	0	0.07	0.07	13.03	0	0	0	0	6.57	0.07	6.50	0
O_2 (lb/hr)	0	0	0	0	11.57	0	0	0	0	0	0	0
CH_4 (lb/hr)	0	0.001	0.001	0	0	0	2.25	2.25	5.15	5.15	0	2.89

Table 4.0.2. Overall Process Stream Table of Atmospheric Feed, Martian Ice Feed, and Inerts

Streams	**Atmospheric Feed**	**Martian Ice Feed**	**Inerts**
Phase	Vapor	Solid	Vapor
Temperature (℉)	-63.67	-76	-159.07
Pressure (psi)	0.116	13.7	4.21
CO_2 (lb/hr)	11.18	0	3.24
H_2O (lb/hr)	0	15.6013	0
N_2 (lb/hr)	0.127	0	0.127
Ar (lb/hr)	0.154	0	0.154
Salts (lb/hr)	0	3.3094	0

4.1 Atmosphere Separation

The atmospheric separator unit freezes carbon dioxide to separate it from other inert gases, specifically nitrogen and argon, with a cryocooler. A stream table of the cryocooler is shown in Table 4.1.1 below, yet without the trace gases that are also separated from carbon dioxide in this process.

Table 4.1.1. Atmospheric Separator Unit Stream Table

Streams	Atmospheric Feed	Inerts	Pure CO_2 Feed
Temperature (℉)	-63.67	-159.07	-128.24
Pressure (psi)	0.116	4.21	13.7
CO_2 (lb/hr)	11.18	3.24	7.94
N_2 (lb/hr)	0.127	0.127	0.000
Ar (lb/hr)	0.154	0.154	0.000

These gases are taken from the atmosphere directly using a fan at -63.67 ℉ and 0.116 psi, based on atmospheric trends on Mars, and then brought into a freezer chamber. An AFCryo STC90 cryocooler then removes heat from the freezer chamber through contact with a Stirling cold head. The cold head surface collects and stores carbon dioxide at -159.07 ℉ as dry ice, and a vacuum pump pumps out the inert gases, thus requiring that 11.92 kW be removed to cool the gas and then an additional 787.53 W be removed to freeze the gas. The dry ice is heated with 8 cartridge heaters per unit and pressurized to form a vapor at 128.24 ℉, which requires that a total of 798.33 W of heat be added. The vapor carbon dioxide is sent to a tank where it combines with the recycle stream such that the process can begin again. To meet our design requirement of 7.94 lb/hr, our process involves 4 carbon dioxide freezer units. Each unit is 3.13 ft in length, 1.50 ft in

width, 2.08 ft in height, and weighs 340 lb. The total weight of the atmospheric separation unit is 1,360 lb.

4.2 Desalination

The desalination system removes impurities in the form of salts from a Martian ice feed, ultimately producing pure water to be fed into the electrolyzer. Four distinct units are involved, those being two heat exchangers, a vertical flash, and a pump. A stream table of the desalination system is depicted in Table 4.2.1.

Table 4.2.1. Desalination System Stream Table

Streams	**Martian Ice Feed**	**Impure H_2O**	**Pure H_2O**	**Waste Salts**	**Condensed H_2O**	**H_2O Inlet**
Temperature (℉)	-76	68	219.1	219.1	72.5	72.7
Pressure (psia)	13.7	13.7	13.7	13.7	13.7	51.7
H_2O (lb/hr)	15.6013	15.6013	13.0299	2.5714	13.0299	13.0299
Salts (lb/hr)	3.3094	3.3094	0	3.3094	0	0

In terms of the equipment, the first heat exchanger operates at 68 ℉ and 13.7 psia and requires 990.2 W to conduct heating, the vertical flash operates at 13.7 psia with a vapor fraction of 0.8 and requires 4,422.2 W to conduct heating, and the second heat exchanger operates at 72.5 ℉ and 13.7 psia and requires 4,266.7 W to conduct cooling.

4.3 Electrolyzer

A proton exchange membrane (PEM) electrolyzer was selected over an alkaline water electrolyzer because they are not susceptible to corrosion, maintenance is simple, and there are fewer components within a single unit than in the case of alkaline water electrolyzers. These features are all important for maintaining structural integrity on Mars.

The Nel C10 PEM Hydrogen Generation System serves as the basis for the electrolyzer, which has the following properties: a nominal hydrogen production rate of 10 Nm^3/hr, a nominal delivery pressure of 435.1 psia, a power consumption of 6.2 kWh/Nm^3 of hydrogen, and a hydrogen purity of 99.9998%. The deionized water that is fed into the system has a consumption rate of 9 L/hr at maximum hydrogen production, a temperature of roughly 72.5 ℉, and a pressure of 51.7 psia. In terms of mass flow rates, H_2O enters the electrolyzer at 13.03 lb/hr, whereas the H_2 outlet stream involves 1.46 lb/hr of H_2 and the O_2 outlet stream involves 11.57 lb/hr of O_2.

The total weight of the electrolyzer is 6,027 lb, with two connected enclosures with dimensions of 99” x 46” x 79” for the electrolyzer itself and 67” x 41” x 79” for the power supply. The efficiency of the electrolyzer is 57.17%.

4.4 Sabatier Reactor

The Sabatier reactor uses a 0.5 wt% ruthenium on alumina catalyst packed bed to produce the desired methane product. These catalysts are expected to perform with a 76% conversion rate for over 120 hours. The unit is a shell and tube heat exchanger filled with 32 parallel 20” long, 0.7” diameter plug flow reactors made of stainless steel tubing. The total mass of the reactor is 118.46 lb, including the weight of the stainless steel tubes, which is 115.46 lb, and the packed catalysts, which is 3 lb (Hayward Pipe & Supply Co, Inc., n.d.; Stainless Steel Type 304-304L, n.d.). A stream table of the Sabatier reactor is shown in Table 4.4.1.

Table 4.4.1. Sabatier Reactor Stream Table

Streams	**CO_2 Feed**	**H_2 Combined**	**Reactor Products**
Temperature (℉)	662	71	752
Pressure (psi)	13.7	13.7	13.7
H_2 (lb/hr)	0	2.11	0.65
CO_2 (lb/hr)	10.44	0	2.51
H_2O (lb/hr)	0.07	0	6.57
CH_4 (lb/hr)	0.001	2.25	5.15

The Sabatier reactor operates at 13.7 psi and the CO_2 and H_2 is preheated to 662 ^oF before entering the reactor. The reactor produces 3,487.2 W of heat due to the highly exothermic reaction, with an allowed increase in temperature of 90 ^oF to 752 ^oF.

4.5 Dehumidifier System

The dehumidifier is a series of operation units that removes water from the reactor effluent before it enters a separator. This water is then sent into a water collection tank at a purity of 99.99 mol %. The flash drum is 1.9601 ft tall with a volume of 0.36964 ft^3. It is made of nickel alloy to withstand the hot stream temperatures. Therefore, the flash drum weighs 205 lb. A stream table of the dehumidifier process can be found below as Table 4.5.1.

Table 4.5.1. Dehumidifier Stream Table

Streams	**Reactor Products**	**Once Cooled Reactor Products**	**Twice Cooled Reactor Products**	**H_2O to Tank**	**Dehumidifier Outlet**
Temperature (℉)	752	177	35.6	35.6	35.6
Pressure (psia)	13.7	13.7	13.7	13.7	13.7
H_2 (lb/hr)	0.33	0.33	0.33	0.00	0.33
CO_2 (lb/hr)	2.51	2.51	2.51	0.00	2.51
H_2O (lb/hr)	6.54	6.54	6.54	6.50	0.04
CH_4 (lb/hr)	2.89	2.89	2.89	0.00	2.89

4.6 Product Separation and Storage

The products of the reactor, those being carbon dioxide, methane, hydrogen, and trace amounts of water, are separated utilizing a cryogenic distillation column. A stream table of the distillation column can be seen in Table 4.6.1 below. Oxygen does not require separation, but still needs to be liquefied, which is covered in more detail in section 3.7.

Table 4.6.1. Cryogenic Distillation and O_2 Stream Table

Streams	**H_2 Recycle**	**CO_2 Recycle**	**CH_4 to Tank**	**O_2 to Pump**
Temperature (℉)	-234.8	-38.3	-234.8	-245
Pressure (psi)	145	145	145	145
H_2 (lb/hr)	0.649	0.000	0.003	0
CO_2 (lb/hr)	0.003	2.503	0.003	0
H_2O (lb/hr)	0.000	0.053	0.000	0
O_2 (lb/hr)	0	0	0	12
CH_4 (lb/hr)	2.25	0.001	2.894	0

4.7 Heat Exchangers

Some of the heat exchangers in the process function as heaters, while others function as coolers. The characteristics and design specifications of the heaters are included in Table 4.7.1 and the characteristics and design specifications of the coolers are included in Table 4.7.2.

Table 4.7.1. Characteristics and Design Specifications of the Heaters in the Process

Equipment Name	Inlet Stream	Outlet Stream	Inlet Temp (^oF)	Outlet Temp (^oF)	MoC	Duty (W)	Length (ft)	Heat Transfer Area (ft^2)	Mass (lb)
H_2 HX	H_2 Low	Heated H_2 Low	70.8	662	Nickel alloy	874.0	2.0	1.9	2.8
CO_2 HX	Pure CO_2 Feed	Heated Pure CO_2 Feed	-128.2	662	Nickel alloy	409.5	1.0	0.8	1.11
H_2 Recycle HX	H_2 Recycle	Heated H_2 Recycle	-243.7	662	Nickel alloy	950.2	2.0	1.6	0.68
CO_2 Recycle HX	CO_2 Recycle	Heated CO_2 Recycle	-38.5	662	Nickel alloy	248.1	0.5	0.5	0.68
Ice HX	Martian Ice Feed	Impure H_2O	-76.0	68	Nickel alloy	990.2	0.7	0.5	1.86
Reboiler HX	Dry Reactor Products	CO_2 Recycle	-22.0	-38.34	Nickel alloy	940.5	0.5	0.16	1.24

Table 4.7.2. Characteristics and Design Specifications of the Coolers in the Process

Equipment Name	Inlet Stream	Outlet Stream	Inlet Temp (^oF)	Outlet Temp (^oF)	MoC	Duty (W)	Length (ft)	Heat Transfer Area (ft^2)	Mass (lb)
H_2O HX	Pure H_2O	Condensed H_2O	219.1	72.5	Nickel alloy	-4266.7	0.7	0.6	3.85
Cooler 1	Reactor Products	Once Cooled Reactor Products	752.0	163.7	Nickel alloy	-1644.4	1	2.4	27.2
Cooler 2	Once Cooled Reactor Products	Twice Cooled Reactor Products	163.7	35.6	Nickel alloy	-2452.6	2.0	12.2	29.6
Cooler 3	Compressor Outlet	Dry Reactor Products	544.7	-22.0	Nickel alloy	-1028.2	1.0	4.0	10.1
O_2 HX	O_2 to Tank	O_2 to Pump	59	-245	Nickel alloy	-502	0.25	1.51	1.4
Condenser HX	Dry Reactor Products	CH_4 to Tank/H_2 Recycle	-22	-234.8	Nickel alloy	-1515	0.3	0.037	3.87

4.8 Pumps and Compressors

The pumps in our process are embedded in the desalination system and on the final product streams to move the fluids to the tanks. The pump in the desalination system also serves to increase the pressure of that stream before reaching the electrolyzer. The pump being employed for these purposes is the United States Plastic Corp. Medium/High Flow Variable Speed Pump. The compressor in our process increases the pressure of the reactor effluent such that the materials can be liquefied. The compressor being employed is the Ingersoll Rand Electric Air Compressor. The design specifications for the pumps and the compressor are contained in Table 4.8.1, including pressure change, power, and mass.

Table 4.8.1. Design Specifications of the Pumps and the Compressor in the Process

Equipment	Manufacturer	Pressure Change (psia)	Power (kW)	Mass (lb)	Price
H_2O Pump	United States Plastic Corp.	37.98	0.0004	2.9	$916.37
O_2 Pump	United States Plastic Corp.	N/A	0.0004	2.9	$916.37
CH_4 Pump	United States Plastic Corp.	N/A	0.0004	2.9	$916.37
Compressor	Ingersoll Rand	131.3	1.12	425	$1,812.31

4.9 Tanks

The carbon dioxide tank was designed based on its total inlet volumetric flow rate, which is 212.09 ft^3/hr, from the purified CO_2 stream and the CO_2 recycle stream. The carbon dioxide is 662 ℉ and 13.7 psi. The tank uses a 10-minute holding time because it is a short-term storage unit, which makes the volume 35.35 ft^3 and the length and the diameter each 3.56 ft. The inlet and outlet flow rates are displayed in Table 4.9.1.

Table 4.9.1. CO_2 Tank Stream Table

Streams	**Heated Pure CO_2 Feed**	**Heated CO_2 Recycle**	**CO_2 Feed**
Temperature (℉)	662	662	662
Pressure (psi)	13.7	13.7	13.7
CO_2 (lb/hr)	7.94	2.50	10.44
H_2O (lb/hr)	0.00	0.07	0.07
CH_4 (lb/hr)	0.00	0.001	0.001

The tank is made out of aluminum. The thickness of the tank is 0.39 inches, such that it has a mass of 222 lb and a shell volume of 1.32 ft^3. The tank is surrounded by 37 layers of double aluminized Mylar multilayer insulation. The total required energy to insulate the tank is 1.21 W.

The final product storage tanks for both methane and oxygen were determined to be out of the scope of this project as they would be required whether or not rocket fuel was produced on Mars or shipped there.

4.10 Power

Electrical power in the ISRU process is provided by 12 Kilopower nuclear generator units that were designed and developed by NASA. These units use nuclear energy to produce 10 kW of electrical energy.

5. Process Economics

5.1 Mass Costs

The most substantial cost associated with the ISRU process is the mass transport of resources, unit operations, and ancillary equipment from Earth. The total mass of all pipes in the system was estimated to be 12,666.92 lb. This mass includes that for the CO_2 cooling pipes. The remaining mass of all pipes in the system was calculated by approximating it as 20% of the total mass of all of the units in the system, per the recommendation by our advisor. The total mass of the unit operations, ancillary equipment, and consumables is 31,749.62 lb. The masses of the individual items can be seen in Table 5.1.1 through Table 5.1.6 below. As shown in Table 5.1.1, the largest mass cost in the system is associated with the Kilopower nuclear generators. Therefore, it was also deemed important to attempt to reduce the power requirements in the system. Based on the estimation that each pound of material launched from Earth costs $10,000, a total shipping cost of $443,836,868.80 is necessary (Mohon, 2019). Excess consumables and spare parts were considered to be out of the scope of this project, and were therefore not included in the mass costs.

Table 5.1.1. Masses of Unit Operations

Unit Operation Name	**Mass (lb)**
Sabatier Reactor	118.46
Dehumidifier	205.04
Desalinator	1.87
Distillation Column	10.12
Electrolyzer	6,027.44
Liquid Nitrogen Recycle System	3,333.00
Kilopower Nuclear Generators (12)	19,800.00
Atmospheric Capture System (4)	1,360.00
Unit Operation Total:	***30,855.93***

Table 5.1.2. Masses of Pumps and Compressors

Pump or Compressor Name	**Mass (lb)**
H_2O Pump	2.90
O_2 Pump	2.90
CH_4 Pump	2.90
Compressor	425.00
Pumps and Compressor Total:	***433.70***

Table 5.1.3. Masses of Tanks

Tank Name	Mass (lb)
CO_2 Tank	222.20

Table 5.1.4. Masses of Heat Exchangers

Heat Exchanger Name	Mass (lb)
H_2 HX	2.80
CO_2 HX	1.10
H_2 Recycle HX	2.40
CO_2 Recycle HX	0.70
Ice HX	1.86
H_2O HX	3.81
Cooler 1	6.71
Cooler 2	29.63
Cooler 3	10.06
O_2 HX	1.40
Heat Exchanger Total:	***60.47***

Table 5.1.5. Masses of Ancillary Equipment

Equipment	Mass (lb)
Ice Drilling Machine	143.30
Heat Exchanger Insulation Jackets	31.00
Ancillary Equipment Total:	***174.30***

Table 5.1.6. Masses of Consumables

Consumable	Mass (lb)
0.5 wt% Ru on Alumina	3.02

5.2 Power Costs

Costs associated with power consumption are the second most significant in the scheme of this project since there are many energy demanding operations being used. Table 5.2.1 through Table 5.2.5 detail the power requirements of each unit operation, heat exchanger, compressor, pumps, and tank. The total power requirement of the ISRU system is 114,099.85 W and is achieved through the use of 12 Kilopower nuclear generators. Due to the $20 million purchase cost of the Kilopower generators, power costs of the ISRU system amount to $240 million.

Table 5.2.1. Power Requirements of Unit Operations

Unit Operation Name	**Energy (W)**
Dehumidifier	< 1.00
Desalinator	4,423.00
Distillation Reboiler	940.50
Electrolyzer	59,873.52
Liquid Nitrogen Recycle System	30,255.00
Atmospheric Capture System (4)	13,502.53
Unit Operation Total:	***108,994.55***

Table 5.2.2. Power Requirements of Pumps and Compressors

Pump or Compressor Name	Energy (W)
H_2O Pump	0.43
O_2 Pump	0.43
CH_4 Pump	0.43
Compressor	1,130.80
Pumps and Compressor Total:	***1,132.09***

Table 5.1.3. Power Requirements of Tanks

Tank Name	Energy (W)
CO_2 Tank	1.21

Table 5.2.4. Power Requirements of Electric Heat Exchangers

Heat Exchanger Name	Energy (W)
H_2 HX	874.00
CO_2 HX	409.50
H_2 Recycle HX	950.20
CO_2 Recycle HX	248.10
Ice HX	990.20
Heat Exchanger Total:	***3,472.00***

Table 5.2.5. Power Requirements of Ancillary Equipment

Equipment	Energy (W)
Ice Drilling Machine	500.00

5.3 Capital Costs

The bare module costs of the unit operations, heat exchangers, compressor, pumps, and tank in the process were calculated using CAPCOST and are listed in Table 5.3.1 through Table 5.3.6 (Turton et al., 2018). Due to the fact that our process units are often smaller than the minimums CAPCOST allows for, the minimum price offered in CAPCOST was used as a conservative estimate for the bare module cost in such cases. The cost of the ice drilling machine, atmospheric capture system, and liquid nitrogen recycle system were estimated to be roughly $143,000, $1.4 million, and $3.3 million, respectively. Price quotes were not specified on CAPCOST or on manufacturing websites for these units, thus these estimations are based on the assumption that the capital cost of these items likely equals 10% of their liftoff cost, per the recommendation by our advisor. The cost of piping for the entire system, including piping for the ambient CO_2 cooler, amounts to $454,202, based on the assumption that piping is roughly 5% of the total equipment cost, per the recommendation by our advisor. The cost of consumables for the process is $6,847.85, based on price quotes from Sigma-Aldrich (Sigma-Aldrich, n.d). Excess consumables and spare parts were considered to be out of the scope of this project, and were therefore not included in the capital costs. The total capital costs for the system amount to $9,538,241.96.

Table 5.3.1. Capital Costs of Unit Operation Equipment

Unit Operation Name	Bare Module Cost ($)
Sabatier Reactor	73,200.00
Dehumidifier	122,000.00
Desalinator	40,500.00
Distillation Column	828,000.00
Electrolyzer	44,200.00
Liquid Nitrogen Recycle System	3,333,000.00
Atmospheric Capture System (4)	1,360,000.00
Unit Operation Total:	***5,800,900.00***

Table 5.3.2. Capital Cost of Pumps and Compressors

Pump or Compressor Name	Bare Module Cost ($)
H_2O Pump	916.37
O_2 Pump	916.37
CH_4 Pump	916.37
Compressor	2,840,000.00
Pumps and Compressor Total:	***2,842,749.11***

Table 5.3.3. Capital Cost of Tanks

Tank Name	Bare Module Cost ($)
CO_2 Tank	77,700.00

Table 5.3.4. Capital Cost of Heat Exchangers

Heat Exchanger Name	Bare Module Cost ($)
H_2 HX	17,800.00
CO_2 HX	17,800.00
H_2 Recycle HX	17,800.00
CO_2 Recycle HX	17,800.00
Ice HX	23,200.00
H_2O HX	23,200.00
Cooler 1	23,200.00
Cooler 2	24,000.00
Cooler 3	23,200.00
O_2 HX	23,200.00
Heat Exchanger Total:	***211,200.00***

Table 5.3.5. Capital Cost of Ancillary Equipment

Equipment	Bare Module Cost ($)
Ice Drilling Machine	143,000.00
Heat Exchanger Insulation Jackets (31)	1,643.00
Ancillary Equipment Total:	***144,643.00***

Table 5.3.6. Capital Cost of Consumables

Consumable	Bare Module Cost ($)
0.5 wt% Ru on Alumina	6,847.85

5.4 Labor Costs

The most significant operational cost associated with our process is that of astronaut labor. Based on the time value of astronauts being $130,000 per hour, as well as the trip being designed for a four astronaut team with 80 hours of set-up time and 533 hours of downtime maintenance, the cost of astronaut labor amounts to $110,890,000 (Johnson, 2019).

For the rest of the cycle, the plant is operated remotely from Earth. The unit operations are designed to send data in real time to Earth for operators to interpret and act upon. Realistically, there would be some time delay, but this could possibly be mitigated by the allotted 10-minute holding time in the CO_2 tank. The design of the transmission technology is the responsibility of specialists in other engineering disciplines, and therefore was assigned to be out of the scope of this project. This team of remote operators comprises six engineers. Due to the continuous nature of this process, two operators work at a time in 8 hour shifts. Assuming each operator is paid at a rate of $100 per hour, the cost of the remote operators over one cycle amounts to $995,000, bringing the total labor costs to $111,885,000.

5.5 Overall Cost Analysis Conclusions

With labor, power, capital, and mass costs calculated, we can begin to compare the overall cost of producing methane, oxygen, and water using an ISRU system to the cost of shipping those resources to Mars. Due to the production of potable water as a byproduct of the Sabatier reaction, different economic analyses can be performed based on whether water is considered a valuable product. Different scenarios can also be constructed due to ISRU's capacity to last for more than one cycle, allowing for the cost comparison of ISRU and fuel transportation across multiple years. Scenario 1 through scenario 4 detail the cost breakdown of different possibilities within this project. Scenario 1 and scenario 2 discuss fuel transportation costs compared to utilizing ISRU for one cycle, showing the difference in cost-efficiency when considering water liftoff costs. Scenario 3 and scenario 4 discuss the cost breakdown across two cycles rather than one, clearly showing that ISRU becomes more cost-efficient in the long term, saving up to $1.2 billion in just one additional cycle.

Scenario 1

NASA has already created efficient methods of reclaiming potable water from wastewater aboard the ISS. The Urine Processor Assembly was designed in 1990 and employs distillation, filtration, and chemical applications to produce potable water from astronaut waste (Mohon, 2020). For this reason, this scenario is a cost comparison that ignores the production of water, since processes like the Urine Processor Assembly may render the shipment of drinking water irrelevant. Without considering the liftoff costs of water, ISRU would cost more than transporting fuel for one trip, losing $85 million. Table 5.5.1 shows the economic comparison between fuel transportation and ISRU without the consideration of potable water for one cycle.

Table 5.5.1. Cost Comparison of ISRU and Fuel Transportation without Water

ISRU		**Fuel Transportation**	
Mass Costs	$443,836,868.80	Methane Shipping Cost*	$144,000,000.00
Power Costs	$240,000,000.00	Methane Purchase Cost*	$8,840.00
Capital Costs	$9,538,241.96	Oxygen Shipping Cost	$576,000,000.00
Labor Costs	$111,885,000.00	Oxygen Purchase Cost**	$3,927.00
Total Cost:	***$805,260,110.76***	***Total Cost:***	***$720,012,767.00***

* Methane was priced at $0.89/lb (Dinkin, 2016).

** Oxygen was priced at $0.05/lb (Wade, n.d.).

Scenario 2

The second scenario is a cost comparison that includes the savings resulting from the production of water as a byproduct of the Sabatier reaction. This water could be used to reduce the amount of ice mining necessary for the reaction, ultimately decreasing the power requirements and liftoff cost of the process. These considerations, however, were left for future research, so this scenario considers the water that is produced as being used for astronaut consumption. The consideration of the production of water in ISRU is the determining factor for a cost saving conclusion in one cycle, with this scenario saving $238 million. Table 5.5.2 shows the economic comparison between ISRU with water deemed a valuable resource and the shipment of the same amount of water from Earth for one cycle.

Table 5.5.2. Cost Comparison of ISRU and Fuel Transportation with Water

ISRU		**Fuel Transportation**	
Mass Costs	$443,836,868.80	Methane Shipping Cost	$144,000,000.00
Power Costs	$240,000,000.00	Methane Purchase Cost	$8,840.00
Capital Costs	$9,538,241.96	Oxygen Shipping Cost	$576,000,000.00
Labor Costs	$111,885,000.00	Oxygen Purchase Cost	$3,927.00
		Water Shipping Cost*	$323,375,000.00
Total Cost:	***$805,260,110.76***	***Total Cost:***	***$1,043,387,767.00***

* This was based on a water collection rate of 6.5 lb/hr, as seen in Table 4.4.1, as well as an assumption that water capital costs are negligible compared to liftoff costs.

Scenario 3

Scenario 3 details the case in which ISRU is established for two cycles, which would save $564 million compared to fuel transport. This is because the liftoff, capital, and power costs would remain effectively unchanged, with the main increase being in labor costs due to the remote operators and astronauts. On the other hand, costs associated with fuel transport would double for every cycle. Table 5.5.3 shows the scenario in which ISRU is established for two cycles compared to shipping enough fuel for two return trips.

Table 5.5.3. Cost Comparison of ISRU and Fuel Transportation without Water for Two Trips

ISRU		**Fuel Transportation**	
Mass Costs	$443,873,108.80	Methane Shipping Cost	$288,000,000.00
Power Costs	$240,000,000.00	Methane Purchase Cost	$17,680.00
Capital Costs	$9,545,089.81	Oxygen Shipping Cost	$1,152,000,000.00
Labor Costs	$182,170,000.00	Oxygen Purchase Cost	$7,854.00
Total Cost:	***$875,588,198.61***	***Total Cost:***	***$1,440,025,534.00***

Scenario 4

Scenario 4 is the case in which ISRU is established for two cycles and water liftoff costs are considered. This scenario is the most cost-efficient case, saving nearly $1.2 billion. Table 5.5.4 shows the scenario in which ISRU is established for two cycles compared to shipping enough fuel for two return trips.

Table 5.5.4. Cost Comparison of ISRU and Fuel Transportation with Water for Two Trips

ISRU		**Fuel Transportation**	
Mass Costs	$443,873,108.80	Methane Shipping Cost	$288,000,000.00
Power Costs	$240,000,000.00	Methane Purchase Cost	$17,680.00
Capital Costs	$9,545,089.81	Oxygen Shipping Cost	$1,152,000,000.00
Labor Costs	$182,170,000.00	Oxygen Purchase Cost	$7,854.00
		Water Shipping Cost	$646,750,000.00
Total Cost:	***$875,588,198.61***	***Total Cost:***	***$2,086,775,534.00***

6. Safety & Environmental Considerations

Considering the dangers seen in the past with regard to sending people and materials into space, safety is a significant factor in designing this process. Furthermore, a failure of the plant could be catastrophic if there are astronauts on the planet that are relying on the fuel produced to return back to Earth. The most important chemical safety concerns surround the incompatibilities of the materials used in this process. Through running a compatibility analysis using CAMEO Chemicals, it is apparent that the largest notable incompatibilities are between oxygen and hydrogen, which can be explosive, flammable, and generate gas or heat. These materials will be controlled in our electrolyzer but having redundant safety systems in play, particularly with a safety integrity level of 3 for emergency shutdown systems, is necessary. This would entail a redundant system for the sensor, logic solver, and final control level (Louvar & Crowl, 2019). The incompatibility hazards are similar for oxygen and methane, but with the assumed efficiency of nearly 100% for separating the exiting hydrogen and oxygen streams of the electrolyzer, these materials will not come into contact in this process. Still, designing the plant to have streams with these two materials far apart is essential. This should also include assurance that there is no way for methane and oxygen to come into contact with each other even given a pipe leakage of one or both of these materials.

In order to control static electricity from interactions between conductive materials in this process, such as gas-solid and liquid-liquid interfaces, all of the unit operations and reactors should be grounded (Louvar & Crowl, 2019). Before loading and after unloading the catalysts in the Sabatier reactor and after any internal repairs or modifications, the equipment should be thoroughly cleaned to prevent contamination and potential hazards or failures in the reactor (European Catalyst Manufacturers Association, 2018). It could also be beneficial to look into

artificial intelligence technologies. For example, the Mars rover has a weather prediction model, which could be implemented into our process to allow for better temperature control of the instrumentation (*Curiosity rover*, 2017). Using AI could allow for auto calibration of the unit to fix drifts and react and adjust to minor incidents. The design of the AI is considered to be out of the scope of this project, but it could be helpful in ensuring more people will not need to be sent to space to perform simple maintenance on the process.

It is important to understand the differences between Earth and Mars when considering the environmental factors in this process. Groups like the Committee on Space Research (COSPAR) have created measures that address the importance of avoiding the contamination of celestial bodies, also known as forward contamination, as well as changes to the environment of Earth as a result of travel between Earth and other celestial bodies, also known as background contamination (Coustenis et al., 2019). It is necessary to keep planetary contamination policies in mind when designing this process to prevent environmental damage to the Earth and Mars, and many studies are being conducted by groups like COSPAR to determine the best ways to do so. Furthermore, there are ethical concerns about polluting another planet as the environmental damage pollution has done to Earth is clear and considerable. Our waste streams only consist of argon, nitrogen, and other trace gases already found in the atmosphere of Mars and waste salts already found in Martian soil, so the effect of pollution from our waste streams is not a serious concern.

The ice drilling system that is used for this process could be another environmental issue as drilling and mining are known to have negative effects on Earth environmentally. The habitat for the astronauts could also have significant impacts on the Martian environment, as it would be designed to emulate an Earth-like space that would be drastically different from that of Mars.

The design of this habitat is considered to be out of the scope of this project, as are the environmental considerations surrounding it. Notably, the generators for this process run on nuclear power, so they are relatively safe and renewable.

7. Social Considerations

The social considerations of our project largely relate to the advantages and disadvantages of a manned Mars mission in general. From exploratory, educational, and economic standpoints, embarking on such an expedition can be defended. However, there are also significant challenges associated with a manned Mars mission that call into question the justifiability of the project from a societal lens.

In terms of exploration, a greater volume of scientific data is able to be collected when humans are incorporated into a Mars mission. For instance, the Spirit and Opportunity rovers launched by NASA in 2004 each carried just five scientific instruments and a rock abrasion tool (*Mars Exploration*, n.d.). In contrast, it is estimated that between tens and hundreds of pieces of equipment could be operated by a single astronaut, far surpassing the half dozen capacity per NASA rover (Ehlmann et al., 2005).

In terms of education, the United States has been characterized by a decrease in the production of scientists and engineers in recent years. Data suggest that the number of PhDs earned in such disciplines is positively correlated with a rising NASA budget (Ehlmann et al., 2005). Further, the initiation of the Apollo program in the 1960s under President Kennedy's administration was likely responsible for the upsurge in the number of American students pursuing advanced degrees in science, math, and engineering in the immediate aftermath (Ehlmann et al., 2005). As such, a manned Mars mission in modern times could similarly serve as inspiration for entering these fields.

In terms of economics, technological developments spurred by a manned Mars mission would likely induce gains in the U.S. market share, produce new markets, cause resources to be used more productively, expand business, and create high-wage jobs (Ehlmann et al., 2005).

Moreover, the following serve as challenges associated with a manned Mars mission: harmful effects of microgravity and radiation on human health; limited air, water, and food resources; limited energy supply; threat to human safety and health in space; and hardware impairment by extreme conditions of space (Ehlmann et al., 2005). These dangers necessitate technical innovation for the purpose of combating them. In particular, the following areas of technological development present an opportunity for advancement related to the aforementioned challenges, respectively: pharmacological and mechanical prevention treatments; closed loop life-support systems; alternative energy sources for low energy-use technologies; automation and robotics; and extended life and low maintenance materials, hardware, and systems (Ehlmann et al., 2005).

A considerable disadvantage of a manned Mars mission is related to its feasibility. Estimates from the Science & Technology Policy Institute posit that the departure date for such an expedition through NASA would be impossible by 2033 given all budget scenarios and technology development and testing schedules (Linck et al., 2019). Beyond NASA, many companies and governments are disinterested in investing in a manned Mars mission because profitability in the long-term is uncertain and in the short-term is unrealistic (Kwon & Klein, 2019). Perhaps the most convincing argument against any form of exploration on Mars, however, is that the funds required could instead be invested in solving critical problems on Earth such as climate change, as 62% of American adults believe (Kwon & Klein, 2019).

8. Conclusions & Recommendations

Conclusions

This ISRU process design attempts to resolve the economic and safety issues that arise from shipping all of the rocket fuel and potable water necessary for a one-cycle stay on Mars. One cycle amounts to roughly eight months on the planet, not including downtime and hours devoted to set-up. Our design uses an electrolyzer to obtain oxygen from the water and reacts the remaining hydrogen with carbon dioxide obtained from the atmosphere to form methane within a Sabatier reactor. Potable water is a byproduct of this reaction, and as such it was considered in the economics section when examining the value of its recovery.

The implementation of this process design costs roughly $85 million more than fuel transportation in the case where water is not considered a monetarily valuable resource. On the other hand, if the water that is produced in this process is considered valuable, then roughly $238 million is saved in one cycle. In any case, cost savings were found to only grow with time. The ISRU design is intended to survive for more than one cycle, therefore only the costs of labor and consumables would increase in subsequent cycles, whereas shipping costs would double for fuel transportation.

The social and environmental implications of such an undertaking would be influential to all of mankind. With an establishment on Mars, humans could look further into the cosmos to learn more about the history of the universe we live in, as well as the future possibilities of extraterrestrial colonization. In addition to this, the undertaking of this ISRU process could spark another era of innovation, increasing education rates and job opportunities. Safety and environmental concerns stand as obstacles to this project, with forward and background contamination being of major concern.

Recommendations

A recommendation concerning the product separations is to employ pressure-swing adsorption. Our group initially ruled it out as too costly due to the difficulty of separating methane from hydrogen, but it may be cost-effective as distillation has such a high energy demand, specifically with regard to the significant costs associated with powering liquid nitrogen cooling. This could also be applied to the atmospheric cryocooler unit. A pressure-swing adsorber may be able to accomplish the same separation with less power and cooling requirements. This technology was not originally considered because it is more complex and more difficult to implement. Running the reactor at higher single pass efficiencies could also help with separation energy costs as the hydrogen in the product stream greatly increases the cooling required. A larger single pass efficiency would reduce the energy required to reheat the recycle streams. More heat integration could be possible, but our group anticipated that adding heat exchangers to change the temperatures of small streams like the recycle stream would introduce unnecessary complications for little gain in our process, along with more failure points in the system.

In terms of equipment selection, the electrolyzer in our process is based on the Nel C10 PEM Hydrogen Generation System. This piece of equipment has a mass of 6,027 lb and a power requirement of 59,873 W, thereby demanding significant liftoff and power costs. Further, the electrolyzer is characterized by an efficiency of just 57.17%, so it is recommended that the design be improved in such a manner as to decrease associated costs and increase efficiency.

More research could be done into the material selections for the unit operations used in this process. Most of the design materials were chosen based on their utilization by prominent space agencies like NASA in similar systems. However, it is possible that other materials are

lighter, which would reduce liftoff costs, or more durable, which could allow the process to run for more cycles without requiring maintenance or the replacement of any parts. Increasing the number of cycles that the process runs for without intervention would drastically improve the economic benefits of our design.

9. Acknowledgements

We would like to thank our advisor, Professor Eric Anderson of the Chemical Engineering Department, for his continuous support and assistance throughout our project. Our team would also like to thank Professor Ronald Unnerstall of the Chemical Engineering Department for his advice and expertise related to safety considerations. Most importantly, we would like to thank Taco Bell for the food and sustenance which supported the physical and emotional well-being of the team through the toughest moments of this capstone project.

10. References

Allison, P. (2016, May 18). *How much does a bottle of water cost on the International Space Station?* Alphr. https://www.alphr.com/space/1003486/how-much-does-a-bottle-of-water-cost-on-the-international-space-station/#:~:text=Each%20supply%20trip%20carries%20up,water%20reserves%20of%20the%20ISS

Basic Hydrogen Properties. (n.d.). Hydrogen Tools. https://h2tools.org/hyarc/hydrogen-data/basic-hydrogen-properties

Blauth, S., Leithäuser, C., & Pinnau, R. (2021). Optimal control of the Sabatier process in microchannel reactors. Journal of Engineering Mathematics, 128(1), 19. doi:10.1007/s10665-021-10134-2

Carta, G. (2020). *Heat and Mass Transfer for Chemical Engineers: Principles and Applications.* McGraw-Hill Education.

Coustenis, A., Hedman, N., & Kminek, G. (2019). The challenge of planetary protection. Room Space Journal of Asgardia, 2(20). https://room.eu.com/article/the-challenge-of-planetary-protection#:~:text=Planetary%20protection%20is%20a%20system,life%20in%20the%20solar%20system.

Crowl, Daniel, A. and Joseph F. Louvar. Chemical Process Safety. Available from: VitalSource Bookshelf, (4th Edition). Pearson Technology Group, 2019.

Curiosity rover gets a boost from artificial intelligence. (2017). Nature, 546(7660), 578–578. https://doi.org/10.1038/d41586-017-00626-6

Dallas, J. A., Raval, S., Gaitan, J. P. A., Saydam, S., & Dempster, A. G. (2020). Mining beyond earth for sustainable development: Will humanity benefit from resource extraction in outer space? Acta Astronautica, 167, 181–188. doi:10.1016/j.actaastro.2019.11.006

Density of Aluminum (n.d.). https://amesweb.info/Materials/Density_of_Aluminum.aspx

Devor, R., Captain, J., & Muscatello, A. (2014). Atmospheric processing module for Mars propellant production. https://doi.org/10.1061/9780784479179.047

Dinkin, S. (2016, January 4). Increasing the profit ratio. The Space Review. https://www.thespacereview.com/article/2893/1#:~:text=Liquid%20methane%20costs%20about%20%241.35,which%20fuel%20will%20be%20cheaper

Dudzinski, L (n.d.). Power and Thermal Systems. National Aeronautics and Space Administration. https://rps.nasa.gov/power-and-thermal-systems/power-systems/

Ehlmann, B. L., Chowdhury, J., Marzullo, T. C., Eric Collins, R., Litzenberger, J., Ibsen, S., … Douglas Grant, F. (2005). Humans to Mars: A feasibility and cost–benefit analysis. Acta Astronautica, 56(9), 851–858. https://doi.org/10.1016/j.actaastro.2005.01.010

Electric Air Compressor: 5 hp, 2 stage, vertical, 60 gal tank, 14 CFM, 240V AC. Grainger. (n.d.). https://www.grainger.com/product/INGERSOLL-RAND-Electric-Air-Compressor-5-4L977?searchBar=true&searchQuery=32499600

European Catalyst Manufacturers Association. (2018). Catalyst handling best practice guide . Cefic. https://www.catalystseurope.org/images/Documents/ECMA1004q_-_Catalyst_handling_best_practice_guide.pdf

Franco, C., Devor, R. W., Snyder, S. J., Petersen, E., & Hintze, P. E. (2019, July 7). Study of Sabatier Catalyst Performance for a Mars ISRU Propellant Production Plant. https://ttu-ir.tdl.org/bitstream/handle/2346/84786/ICES-2019-77.pdf?sequence=1&isAllowed=y

Gscheidle, Christian & Killian, Matthias. (2017). Mars Rover - Limits of Passive Thermal Design.

Guo, Y., Li, G., Zhou, J., & Liu, Y. (2019). Comparison between hydrogen production by alkaline water electrolysis and hydrogen production by PEM electrolysis. *IOP Conference Series: Earth and Environmental Science*, *371*(4). https://iopscience.iop.org/article/10.1088/1755-1315/371/4/042022/pdf

Hayward Pipe & Supply Co, Inc. (n.d.). 1/2" pipe & fitting data. http://www.haywardpipe.com/pipe-sizes/12-pipe/

Heldens, J., Fridh, J., Östlund, J. (2021). On the Characterization of methane in rocket nozzle cooling channels. Acta Astronautica, 186, 337-346. doi:10.1016/j.actaastro.2021.05.034

Hydrogen Production: Electrolysis. (n.d.). U.S. Department of Energy. Retrieved November 30, 2021, from https://www.energy.gov/eere/fuelcells/hydrogen-production-electrolysis

Inclán, B., Rydin, M., & Northon, K. (2020, September 25). NASA Report Details How Agency Significantly Benefits US Economy. National Aeronautics and Space Administration. https://www.nasa.gov/press-release/nasa-report-details-how-agency-significantly-benefits-us-economy

Johnson, M. (2019, May 31). Pricing policy. NASA. Retrieved April 10, 2022, from https://www.nasa.gov/leo-economy/commercial-use/pricing-policy

Junaedi, C., Hawley, K., Walsh, D., Roychoudhury, S., Abney, M., & Perry, J. (2011). Compact and Lightweight Sabatier Reactor for Carbon Dioxide Reduction. In *41st International Conference on Environmental Systems 2011, ICES 2011*. doi:10.2514/6.2011-5033

Kruyer, N., Realff, M., Sun, W., Genzale, C., Peralta-Yahya, P., (2021). Designing the bioproduction of Martial rocket propellant via a biotechnology-enabled in situ resource utilization strategy. Nature Communications, 12(6166). doi:10.1038/s41467-021-26393-7

Kwon, N., & Klein, D. (2019, August 20). *Humans beyond Earth*. Research Association for Interdisciplinary Studies. https://doi.org/10.5281/zenodo.3386283

Legal Information Institute (n.d.). 49 CFR § 195.106 - internal design pressure. Legal Information Institute. https://www.law.cornell.edu/cfr/text/49/195.106

Linck, E., Crane, K. W., Zuckerman, B. L., Corbin, B. A., Myers, R. M., Williams, S. R., Carioscia, S. A., Garcia, R., & Lal, B. (2019, February). *Evaluation of a Human Mission to Mars by 2033*. Institute for Defense Analyses. https://www.ida.org/-/media/feature/publications/e/ev/evaluation-of-a-human-mission-to-mars-by-2033/d-10510.ashx

Mace, M., Anderson, E. (advisor), & Ferguson, S. (advisor). (2020). Design of an In-Situ Fuel, Oxygen, and Potable Water Supply System on Manned Mars Missions; Applying Multilevel Perspective Analysis to Energy Justice in India. Charlottesville, VA: University of Virginia, School of Engineering and Applied Science, BS (Bachelor of Science), 2020. doi:10.18130/v3-4vy4-s536

Mars Exploration Rovers. (n.d.). National Aeronautics and Space Administration. https://mars.nasa.gov/mars-exploration/missions/mars-exploration-rovers/

Mason, L., Gibson, M., & Poston, D. (2013). *Kilowatt-class fission power systems for science and Human Precursor Missions- NASA*. https://ntrs.nasa.gov/api/citations/20140010823/downloads/20140010823.pdf

Medium/High Flow Variable-Speed Pump - 4.0 to 600 mL/minute. (n.d.). United States Plastic Corp. https://www.usplastic.com/catalog/item.aspx?itemid=32997

Meier, A. J., Grashik, M., Shah, M., Sass, J., Bayliss, J., Hintze, P., & Carro, R. (2018, September). Full-Scale CO2 Freezer Project Developments for Mars Atmospheric Acquisition. 2018 AIAA SPACE and Astronautics Forum and Exposition. https://doi.org/10.2514/6.2018-5172

Mohon, L. (2019, December 17). *NASA Marshall Achievements celebrated at Alabama Bicentennial Finale*. NASA. Retrieved April 10, 2022, from

https://www.nasa.gov/centers/marshall/news/news/releases/2019/nasa-marshall-achievements-celebrated-at-alabama-bicentennial-commemoration.html

Mohon, L. (2020, October 8). *NASA Marshall engineers refine space station's Urine Recycling System*. NASA. Retrieved April 10, 2022, from https://www.nasa.gov/centers/marshall/news/releases/2020/nasa-marshall-engineers-refine-hardware-apply-innovative-solutions-to-more-reliably-recycle.html

Moioli, E., & Züttel, A. (2020). A model-based comparison of Ru and Ni catalysts for the Sabatier reaction. *Sustainable Energy Fuels*, *4*(3), 1396–1408. doi:10.1039/C9SE00787C

Molecular Sieves: Lithium X. (n.d.). Zeochem. Retrieved November 28, 2021, from https://www.zeochem.com/our-products/molecular-sieves

Mosher, D. (2018, May 3). *NASA built and tested a 'truly astounding' nuclear reactor that may help astronauts travel longer, farther, and faster in space*. Business Insider.https://www.businessinsider.com/nasa-nuclear-reactor-kilopower-how-it-works-2018-5

Multi Layer Insulation (MLI) Vacuum Insulation (n.d.). Meyer Tool & Mfg. https://www.mtm-inc.com/multi-layer-insulation.html

NASA. (2018). Kilopower Press Conference. https://www.nasa.gov/sites/default/files/atoms/files/kilopower_media_event_charts_16x9_fi nal.pdf

NASA's Perseverance Rover Collects Puzzle Pieces of Mars' History. (2021, September 10). National Aeronautics and Space Administration. Retrieved November 30, 2021, from https://mars.nasa.gov/news/9036/nasas-perseverance-rover-collects-puzzle-pieces-of-mars-history/

NASA Phoenix Mars Lander Confirms Frozen Water. (2008, June 20). National Aeronautics and Space Administration. Retrieved November 30, 2021, from https://www.jpl.nasa.gov/news/nasa-phoenix-mars-lander-confirms-frozen-water

National Center for Biotechnology Information (2021). PubChem Compound Summary for CID 297, Methane. https://pubchem.ncbi.nlm.nih.gov/compound/Methane

National Center for Biotechnology Information (2021). PubChem Compound Summary for CID 783, Hydrogen. 16 https://pubchem.ncbi.nlm.nih.gov/compound/Hydrogen

Nel C Series Proton Exchange Membrane (PEM) Hydrogen Generation Systems. (2021). Nel Hydrogen. https://96e597bb58d206f85397.b-cdn.net/wp-content/uploads/2022/01/C-Series-Rev-H.pdf

Niels Bohr Institute (n.d.). Ice on Mars. Copenhagen, Denmark: Centre for Ice and Climate; University of Copenhagen. https://www.iceandclimate.nbi.ku.dk/research/ice_other_planets/ice_on_mars/

Pan, M., Omar, H. M., & Rohani, S. (2017). Application of Nanosize Zeolite Molecular Sieves for Medical Oxygen Concentration. *Nanomaterials (Basel, Switzerland), 7(8)*, 195. doi:10.3390/nano7080195

Peters, M. S., Timmerhaus, K. D., & West, R. E. (2003). *Plant Design and Economics for Chemical Engineers*. McGraw-Hill.

Platcha, D., Feller, J., Johnson, W., & Robinson, C. (2017, February 1). *Liquid nitrogen Zero BOILOFF testing - NASA technical reports server (NTRS)*. NASA. from https://ntrs.nasa.gov/citations/20170001537

Portree, D. S. F. (2013, April 15). Mars Direct: Humans to Mars in 1999! (1990). Wired. Retrieved from https://www.wired.com/2013/04/mars-direct-1990/

Product Specification. (n.d.). Sigmaaldrich.com. https://www.sigmaaldrich.com/specification-sheets/124/829/206199-BULK_____ALDRICH__.pdf

Propellants. (n.d.). National Aeronautics and Space Administration. Retrieved November 30, 2021, from https://history.nasa.gov/conghand/propelnt.htm#:~:text=Liquid%20oxygen%20is%20the%20standard,cause%20fire%20or%20an%20explosion.

Redd, T. (2017, November 17). How Long Does It Take to Get to Mars? Space. Retrieved from https://www.space.com/24701-how-long-does-it-take-to-get-to-mars.html

Ross, R. G. (2015). Quantifying MLI Thermal Conduction in Cryogenic Applications from Experimental Data. IOP Conference Series: Materials Science and Engineering, 101, 012017. https://doi.org/10.1088/1757-899x/101/1/012017

Ruthenium on alumina Sigma-Aldrich. (n.d.). Retrieved April 10, 2022, from https://www.sigmaaldrich.com/CA/en/product/aldrich/206199

Shekhtman, L. (2019, November 13). With Mars Methane Mystery Unsolved, Curiosity Serves Scientists a New One: Oxygen. National Aeronautics and Space Administration. https://www.nasa.gov/feature/goddard/2019/with-mars-methane-mystery-unsolved-curiosity-serves-scientists-a-new-one-oxygen

SpaceX Raptor – spacex: Spaceflight101. Spaceflight101. (n.d.). Retrieved from https://spaceflight101.com/spx/spacex-raptor/.

Stainless Steel Type 304-304L. (n.d.). Rolled Metal Products | Stainless, Aluminum & Specialty Alloys. https://rolledmetalproducts.com/stainless-steel-type-304-304l/

Stull, Daniel R.. (1947). Vapor pressure of pure substances. organic and inorganic compounds, *Ind. Eng. Chem., 4*(39), 517-540. doi:10.1021/ie50448a022.

Thomasnet (n.d.). *All About 6061 Aluminum (Properties, Strength and Uses)*. https://www.thomasnet.com/articles/metals-metal-products/6061-aluminum

Turton, R., Shaeiwitz, J. A., Bhattacharyya, D., & Whiting, W. B. (2018). *Analysis, synthesis, and design of Chemical Processes*. Pearson Education, Inc.

Vogt, C., Monai, M., Kramer, G. J., Weckhuysen, B. M. (2019). The Renaissance of the Sabatier Reaction and Its Applications on Earth and in Space. *Nature Catalysis*, *2*(3), 188–197. doi:10.1038/s41929-019-0244-4.

Wade, M. (n.d.). LOX. Astronautix. Retrieved from http://www.astronautix.com/l/lox.html

Wankat, P. C. (2012). *Separation process engineering: Includes mass transfer analysis* (3rd ed). Prentice Hall.

Water. (2021). NIST Chemistry WebBook. https://webbook.nist.gov/cgi/cbook.cgi?ID=C7732185&Mask=2

Williams, D. R. (2015, December 15). A Crewed Mission to Mars…. National Aeronautics and Space Administration. Retrieved from https://nssdc.gsfc.nasa.gov/planetary/mars/marslaun.html

Xsens (n.d.). Robotic mining competition for NASA Mars Mission. Retrieved from https://www.xsens.com/cases/nasa-mars-mission

Zubrin, R. (2000). The Mars Direct Plan. Scientific American, 282(3), 52–55. Retrieved from http://www.jstor.org/stable/26058636.

Appendix A: Sample Calculations

$$\boldsymbol{Theoretical\ consumption} = -285.83 \frac{kJ}{mol\ H_2O}$$

$$\boldsymbol{Actual\ consumption}$$
$$= \frac{68.9\ kWh}{1\ kg\ H_2} \times \frac{1\ kg\ H_2}{1000\ g\ H_2} \times \frac{2.02\ g\ H_2}{1\ mol\ H_2} \times \frac{2\ mol\ H_2}{2\ mol\ H_2O} \times \frac{1\ kJ}{2.78 \times 10^{-4}\ kWh}$$
$$= 499.97 \frac{kJ}{mol\ H_2O}$$

$$\boldsymbol{Efficiency} = \frac{|Theoretical\ consumption|}{Actual\ consumption} \times 100\% = \frac{|-285.83 \frac{kJ}{mol\ H_2O}|}{499.97 \frac{kJ}{mol\ H_2O}} \times 100\%$$
$$= 57.17\%$$

Figure A.1. Electrolyzer Efficiency Calculations

$$\boldsymbol{Reynolds\ (for\ packed\ beds)} = \frac{\rho u_{bs} D_{EF}}{\mu(1-\varepsilon)}$$

$$u_{bs} = \frac{\left(13.05 \frac{m^3}{hr}\right)}{(32\ pipes)\pi(.0089m)^2(\frac{3600s}{hr})} = 0.46\ m/s$$

$$\varepsilon = \frac{pore\ volume}{total\ volume} = \frac{125.44\ cm^3 - 10.84\ cm^3}{125.44\ cm^3} = 0.9136$$

$$\boldsymbol{Reynolds\ (for\ packed\ beds)} = \frac{\frac{.29\ kg}{m^3} * \frac{.46\ m}{s} * .0032\ m}{2.464 \times 10^{-5}(1-.9136)} = 2.0 \times 10^2$$

$$\boldsymbol{Ergun\ equation}: f_p = \frac{150}{Re_p} + 1.75 = \frac{150}{2.0 \times 10^2} + 1.75 = 2.5$$

$$l_w = f_p \frac{L(1-\varepsilon)}{D_{EF}\varepsilon^3} u_{bs}^2 = 9.3\ \frac{m^2}{s^2}$$

$$\Delta P = -l_w \rho = 9.3\ \frac{m^2}{s^2} * \frac{.29\ kg}{m^3} = 2.71\ \frac{kg}{s^2 m}\ (Pa)$$

$$\Delta P = -3.9 \times 10^{-4}\ psi$$

Figure A.2. Packed Bed Reynolds Number and Pressure Drop Calculations